

A STUDY OF THERMALLY STIMULATED
LUMINESCENCE IN STANNIC OXIDE

By

ROBERT DON EAGLETON

Bachelor of Science
Abilene Christian College
Abilene, Texas
1959

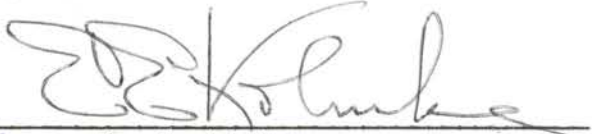
Master of Science
Oklahoma State University
Stillwater, Oklahoma
1962

Submitted to the Faculty of the Graduate College
of the Oklahoma State University
in partial fulfillment of the requirements
for the Degree of
DOCTOR OF PHILOSOPHY
May, 1969

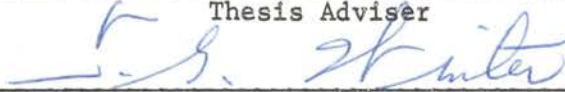
SEP 29 1969

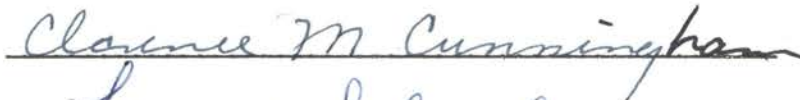
A STUDY OF THERMALLY STIMULATED
LUMINESCENCE IN STANNIC OXIDE

Thesis Approved:



Thesis Adviser









Dean of the Graduate College

724814

ACKNOWLEDGMENTS

The author wishes to state his appreciation to his friends, associates and others for their assistance during the course of this study. He is most grateful to Dr. E. E. Kohnke for his supervision and guidance throughout the course of this research and for the special care taken in the preparation of this thesis. Gratitude is also expressed to Dr. D. L. Rutledge, Dr. C. M. Cunningham, Dr. R. D. Freeman, Dr. K. E. Ebner, and Dr. P. A. McCollum for making available certain apparatus without which this study could not have been possible. The author wishes to express his thanks to fellow members of the research group for their suggestions, information, and the preparation of some of the samples used in this study. Financial support was obtained from several sources through the Oklahoma State University Research Foundation. The author wishes to express his appreciation to the Physics Department for stipend support and for funds made available through a National Defense Education Act Fellowship. Finally he wishes to thank his wife, Barbara, for her encouragement and support throughout the course of this investigation.

TABLE OF CONTENTS

Chapter	Page
I. INTRODUCTION.	1
A Resume of Stannic Oxide Studies.	1
The Historical Development of Luminescence Studies	2
Scope of Present Study	6
II. THE THEORY AND ANALYSIS OF THERMALLY STIMULATED LUMINES- CENCE	9
Introduction	9
Models for Luminescence Processes.	9
Imperfection Centers	17
Attempt-to-Escape Frequency.	24
Band Models for Thermally Stimulated Luminescence.	27
Correlation of T.S.L. and T.S.C.	35
III. EXPERIMENTAL DETAILS.	37
Samples.	37
Apparatus.	38
Experimental Techniques and Procedures	45
IV. EXPERIMENTAL RESULTS.	48
Introduction	48
Basic T.S.L. Measurements.	49
Analysis of T.S.L. Radiation	55
Excitation Radiation	61
Heat Treatment Studies	61
V. DISCUSSION AND CONCLUSIONS.	66
Introduction	66
Justification of Band Model.	66
Trapping and Recombination Centers	67
Heat Treatment Effects	73
Summary of Model	75
Suggestions for Further Study.	76
BIBLIOGRAPHY.	79

LIST OF TABLES

Table	Page
I. Energy Source and the Name of the Associated Luminescence.	3
II. Information Pertaining to the Glow Curves of Figure 18 . .	59
III. Intensity of Luminescence with E Vector Polarized Parallel and Perpendicular to C-Axis of Single Crystal.	62
IV. Effect of Heat Treatment on the Maximum Luminescence In- tensity of Ceramics.	64
V. Activation Energies of Electron Traps Calculated From T.S.L. Measurements.	70
VI. Activation Energies of Electron Traps Calculated From T.S.C. Measurements.	72

LIST OF FIGURES

Figure	Page
1. Configuration Coordinate Energy Level Diagram (Type I).	11
2. Configuration Coordinate Energy Level Diagram (Type II)	14
3. Simplified Energy Level Diagram for the Band Model.	15
4. Energy Levels of an Anion Vacancy in Different States of Ionization.	19
5. Acceptor and Donor Centers for Various Substitutionals in Stannic Oxide	21
6. Model for Oxygen Gas Adsorbed on Stannic Oxide.	25
7. Energy Band Model with One Recombination Level and Two Electron Trapping Levels.	28
8. T.S.L. Apparatus.	40
9. Circuit Diagram of Photomultiplier Tube Voltage Divider	42
10. Block Diagram of T.S.L. Electronic System	43
11. Photomultiplier Tube Cooling Assembly	44
12. Effect of Excitation Time on Glow Curves.	50
13. Effect of Heat-up Rate on Glow Curves	52
14. Effect of Initial Decay Time on Glow Curves	53
15. Effect of Partial Thermal Decay on Glow Curves.	54
16. Representative Glow Curves of Locally-Grown Single Crystals	56
17. Representative Glow Curves of Corning Single Crystals	57
18. Representative Glow Curves of Ceramics.	58
19. Spectral Distribution of Luminescence Radiation	60
20. Glow Curves for Single Crystal Excited with Different	

LIST OF FIGURES (Continued)

Figure	Page
Spectral Ranges of Radiation.	63
21. Thermally Stimulated Current of Ceramic Sample.	68
22. Energy Level Diagram of Model Proposed for Stannic Oxide. . .	76

CHAPTER I

INTRODUCTION

A Resume of Stannic Oxide Studies

Stannic oxide is a rutile-structured material^{1,2} and is classified as a broad-band semiconductor^{3,4} with a separation between valence and conduction bands of about 4 eV^{5,6,7}. Loch suggests that the four electrons of the 5s and 5p orbitals of the tin atoms are transferred to the 2p oxygen atom orbitals. This in turn implies a 2p valence band and a conduction band which is 5s in character or made up of a mixture of 5s and 5p orbitals.

Electrical and optical properties of several different forms of stannic oxide have been investigated during the past decade by various groups using a variety of techniques. Of particular interest to the work reported here are studies on single crystals using photoelectronic techniques^{7,8}, optical absorption techniques^{5,9}, spin resonance methods¹⁰⁻¹³, and electrical resistivity measurements¹⁴. Some preliminary luminescence observations have also been made^{15,16}.

The more recent work done on ceramic samples has emphasized electrical conductivity and related measurements^{3,8,17,18}. In addition to single crystals and ceramics, stannic oxide thin films¹⁹⁻²⁵, pressed powders²⁶, and natural crystals⁴ have been investigated. A review of much of the work done on stannic oxide may be found in a report made by Marley and MacAvoy²⁷.

Early in 1966 the research group here at Oklahoma State University found that stannic oxide single crystals, ceramics, and gels were capable of producing significant thermally stimulated luminescence. These observations suggested another approach to the study of imperfection levels in stannic oxide using thermoluminescence techniques. Subsequently this investigation was undertaken and the results are presented in this dissertation.

The Historical Development of Luminescence Studies

In order that the phenomenon of thermally stimulated luminescence and its application to the study of solid state materials may be properly understood it is desirable to consider first the process of luminescence in general. Broadly speaking, the term luminescence covers situations where matter generates extranuclear, nonthermal electromagnetic radiation characteristic of the material itself.

When a crystalline material is in thermal equilibrium with its surroundings the energy distribution of the electrons and phonons may be described by Fermi-Dirac and Bose-Einstein statistics respectively. It is the interaction and subsequent energy transitions of these electrons and phonons that give rise to thermal radiation when the substance is in thermal equilibrium. However, if energy is transferred to the crystal by some means other than thermal interaction with its surroundings, the energy distribution of the electrons can no longer be described by equilibrium statistics. In this case the energy distribution of the emitted radiation is significantly altered and it is that radiation in excess of the thermal radiation which is called luminescence radiation. In practice it is normally not difficult to distinguish between the two.

At temperatures below 400°K the thermal radiation lies primarily in the far infrared whereas the longest wavelength luminescence studied thus far lies in the near infrared.

There are two ways in which luminescence radiation is normally classified. One is to classify it according to the type of energy which is absorbed, stored and subsequently transformed into luminescence radiation. Table I gives some of these energy sources and the name of the associated luminescence.

TABLE I
ENERGY SOURCE AND THE NAME OF THE ASSOCIATED LUMINESCENCE

Energy Source	Associated Luminescence
Electromagnetic Radiation	Photoluminescence
High Energy Electrons	Cathodoluminescence
Electrical Potential	Electroluminescence
Mechanical Energy	Triboluminescence
Chemical Energy	Chemiluminescence

It should be noted that the common term "thermoluminescence" is not included in this Table I. The reason for its exclusion is that it is not thermal energy that is absorbed, stored and subsequently released as luminescence. Actually, thermoluminescence refers to a process where thermal energy is responsible for the stimulation or the releasing of stored energy to produce luminescence. A more descriptive term and the one to be adopted in this dissertation is "thermally stimulated luminescence" (T.S.L.).

A second method for classifying luminescence categorizes it according to the way in which luminescence intensity varies with time

and temperature subsequent to the removal of the energy source. When the luminescence decays exponentially with time and is independent of the excitation time and temperature, it is referred to as "fluorescence". If the intensity of the emitted radiation is temperature dependent and decays in some non-exponential manner with time then it is referred to as "phosphorescence"^{28,29,30}. An alternate definition chosen by some has been to call "fluorescence" that radiation produced during the time the sample is being excited and "phosphorescence" that component emitted subsequent to excitation^{31,32}.

The history of luminescence observations and studies date back to the 17th century when Casciarolo of Bologna, Italy, observed a persistent afterglow in a substance which he had made, when it was exposed to daylight. Later (1653) Zecchi noted that the color of this phosphorescence did not change when excited by different colors of light. In 1852, Stokes³³ found that the emitted radiation was less refrangible (had a longer wavelength) than was the exciting radiation. This phenomenon is now referred to as Stokes' shift. Becquerel³⁴ (1867) found that the luminescence behavior of uranyl salts decayed exponentially and hyperbolically with time. Due to the similarity of mathematical relations which described these two decay rates with the mathematical relations describing monomolecular and bimolecular chemical reactions, the terms "bimolecular" and "monomolecular" were given to the hyperbolic and exponential decay processes respectively. These terms are now used to refer to those kinetic processes which are describable in terms of electron transitions within a single center (monomolecular) or in terms of electron transitions between two separated centers (bimolecular).

Theoretical explanations for luminescence were initially developed

by Jablonski³⁵ (1933), Seitz³⁶ (1938) and Mott³⁷ (1939). They applied quantum mechanics and developed models wherein the electrons were assumed to have made transitions between stationary electronic states. Calculations took into account the effect of the crystalline field and the change of nuclear coordinates. This model is called the "configuration coordinate model". In it the electrons remain attached to a single atom during the luminescence process. A later model proposed by Riehl and Schon³⁸ (1939) and Johnson³⁹ (1939) took into account the fact that electrons could be freed from the luminescent centers and move through the crystal giving rise not only to emitted radiation but also to photoconductivity or thermally stimulated currents (T.S.C.). This model is based on the usual energy band theory. Both these models and their corresponding mathematical relations will be developed in more detail in Chapter II.

The specific analysis of T.S.L. was initially made by Urbach⁴⁰ (1926). Later Randall and Wilkins³¹ (1945) showed that there existed a direct relationship between T.S.L. and phosphorescence. Garlick and Gibson⁴¹ (1948) extended the work of Randall and Wilkins to investigate the effect of electron retrapping upon the shape of the glow curves. Their results led them to believe that in the materials they studied many of the electron traps were located near luminescence centers.

Understanding luminescence theory of inorganic solids requires unifying knowledge from several phenomenologically related branches of solid state physics which in turn have their theoretical foundations in quantum theory, electromagnetic theory, and statistical mechanics. Thus it is not surprising to find that its predictive abilities are not quite as good as those of some of the more fundamental areas of solid

state physics.

In spite of the theoretical developments made thus far, most of the analyses of luminescence studies continue to be phenomenological and based upon models developed subsequent to the particular experimental work. What would be desirable is a theoretical understanding of how the crystalline host material interacts with imperfections, making it possible to predict the observed electro-optical properties and identify significant parameters. A good deal of success has been made in this respect with luminophores that appear to be describable in terms of the configuration coordinate model. Systems which require an explanation in terms of the band model are usually more complex and consequently present more theoretical difficulties

Scope of Present Study

The special type of luminescence called thermally stimulated luminescence (T.S.L.) has quite often proved to be useful in studying solid state materials. Because of the particular way in which this luminescence is stimulated by phonons, it permits the development of relatively simple techniques whereby such trapping parameters as activation energy^{31,41,42,43}, attempt-to-escape frequency^{31,44} and trap density distribution^{30,31,45,46} may be determined. In addition it has been a valuable aid in developing models to describe the electron kinetic processes to be associated with T.S.C. or T.S.L. phenomena^{31,41,47,48,49}. By analyzing the luminescence emission spectrum, it is also possible in certain cases to determine the energy location of imperfection levels acting as recombination centers within the energy gap^{47,50}.

Reasons have been given in the preceding section to suggest

that the results of T.S.L. studies may be quite readily combined with information obtained from other techniques used for studying the properties of solids. For example, the correlation between T.S.L. and optical analysis, electron paramagnetic resonance, and electrical conductivity measurements have proved useful in identifying or gaining a better insight into the nature of imperfections responsible for the electro-optical properties of a number of crystalline materials. Merz and Persham⁵¹ used optical absorption and T.S.L. techniques to determine the site symmetry and charge reduction mechanisms of rare earth ions in calcium fluoride. Wertz and Coffman⁵² have used electron spin resonance and T.S.L. measurements to identify Fe^{1+} and Cr^{2+} ions in magnesium oxide as the trapping and recombination centers respectively. Broser, et. al.⁴⁶ were successful in validating the equations which they derived relating photoconductivity and luminescence in crystalline sulfides to excitation time, temperature, and intensity for different physical conditions. By comparing conductivity and T.S.L. measurements, Halperin and Nahum⁵³ showed that the release of trapped holes was responsible for the observed luminescence in type IIb semiconducting diamonds.

Another area in which luminescence studies have been quite fruitful has been in the investigation of ambient atmosphere effects upon the electrical properties of metal oxide semiconductors. Oster and Yamamoto⁵⁴ found that oxygen quenches the luminescence and conductivity of zinc oxide at room temperature. They attribute this to surface trapping of electrons by chemisorbed oxygen. In another instance Kroeger and Dikhoff⁵⁵ have found that oxygen, upon replacing sulfur in zinc sulfide, causes the appearance of a new luminescence peak. By invoking the principle of charge and volume compensation, they concluded that

oxygen ions act as traps and the Zn^{1+} ions are the activator centers.

It is the intent of the research reported here to analyze the luminescence data for variously heat-treated and doped stannic oxide single crystals and ceramics to determine the location of imperfection states in the energy gap, to develop a model for the electron kinetic processes and to attempt an identification of the nature of the imperfections responsible for the various trapping and recombination centers. This will be accomplished by:

- 1) analyzing the T.S.L. data and
- 2) by correlating these data with T.S.C. other photoelectronic measurements.

Chapter III describes the experimental details of this research and the results of the T.S.L. measurements are given in Chapter IV. The analysis of the data and its correlation with other research is presented in Chapter V and a model is proposed to explain the observations.

CHAPTER II

THE THEORY AND ANALYSIS OF THERMALLY STIMULATED LUMINESCENCE

Introduction

As stated in the preceding chapter, the research reported here takes a twofold approach to the analysis of stannic oxide luminescence: 1) analysis of T.S.L. data and 2) correlation of T.S.C. and T.S.L. data. It is the purpose of this chapter to present the theory and associated information necessary for such an analysis and correlation. The procedure will be to first present the models in current use for the explanation of luminescence. These models are the configuration coordinate model^{35,36,37} and the band model^{38,39}. The band model involves transitions between conduction band and imperfection energy states and appears to be the appropriate model for use in description of stannic oxide luminescence. An additional section following that on the band model is given describing various types of imperfections likely to be found in stannic oxide. This is in turn followed by mathematical derivations and analytical techniques for the calculation of activation energies from T.S.L. data. Finally, a brief development of the mathematical relations between T.S.L. and T.S.C. is presented.

Models for Luminescence Processes

There are presently two commonly used models for the description of luminescence phenomena. The first and simpler of the two is the "con-

figuration coordinate model" and the second is the "band model". These two models describe luminescence that is produced by two totally different mechanisms. It may be readily determined in the case of T.S.L. which is more suitable. For reasons which will become apparent when these two models are discussed, electrical conductivity may be readily associated with the band model but is not relevant in the case of the configuration coordinate model. Thus if thermally stimulated conductivity is found to behave in a manner similar to thermally stimulated luminescence, this is a good indication that the band model is appropriate.

Configuration Coordinate Model

In the configuration coordinate model the electrons remain in a particular center throughout the excitation → storage → stimulation → luminescence cycle. A center may consist of a single impurity ion or an impurity ion and the neighboring ions depending upon the degree of interaction. Figures 1 and 2 depict how the energy of an electron in a luminescence center is expected to vary as a function of the distance between adjacent ions for the cases of the center in the ground state and in an excited state. These diagrams are highly simplified from the standpoint that the energy of a center depends upon the relative location of all the ions surrounding the center. If there are N ions constituting a center it would require a $3N$ -dimensional coordinate diagram to describe the energy states of the center. However, the salient features of this model may be satisfactorily understood in terms of a one-dimensional diagram.

Figure 1 is useful in explaining temperature-independent fluorescence decay which is also independent of the excitation time and inten-

sity. In this case electrons are excited by a photon of energy $h\nu \approx E_B - E_A$ into an excited energy state of the center. According to the Franck-Condon principle this transition occurs so rapidly that the ions do not have time to change their lattice spacings. Thus a vertical transition

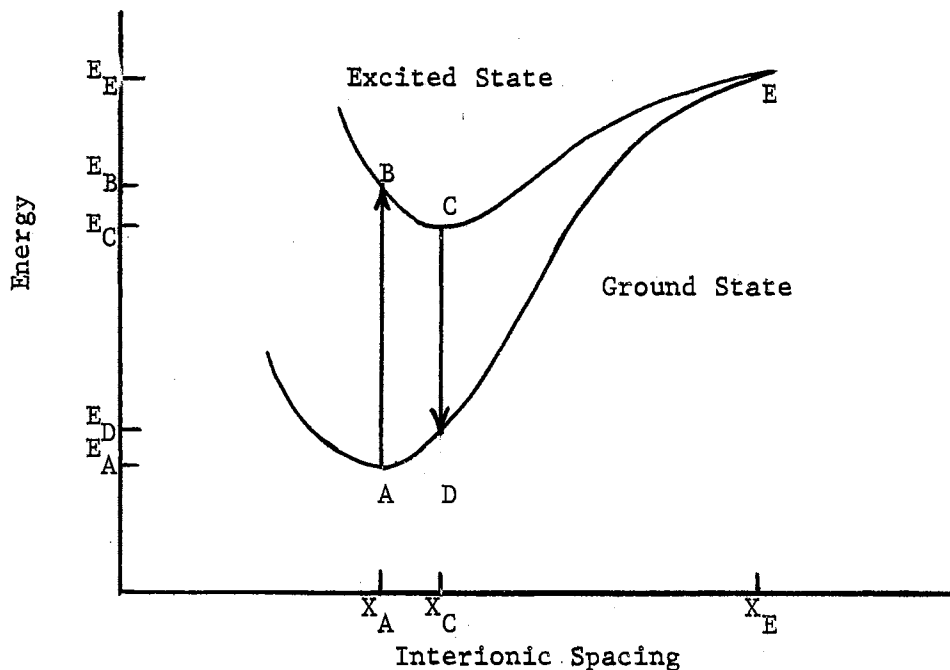


Figure 1. Configuration Coordinate Energy Level Diagram (Type I)

must occur on the configuration coordinate energy level diagram.

Following the excitation the ions take up a new interionic spacing " x_e " which is compatible with the minimum energy for this excited state. The energy difference $E_B - E_C$ is propagated from the center as a phonon.

Assuming the transition from C to D is not forbidden, de-excitation will occur in about 10^{-8} second after excitation. This produces a phonon of energy $E_D - E_A$. Here it is seen that the emitted photon is obviously

less energetic than the incident photon. It is this difference between the incident radiation and the emitted luminescence that is known as the Stokes' shift.

The fluorescence intensity as a function of time is found for the steady state case as follows. Let n_1 and n_2 be the numbers of electrons in the ground and excited states respectively and A_1 and A_2 the rates of excitation and emission respectively. Now the luminescence intensity is proportional to the number of electrons per unit time returning to the ground state,

$$I = CA_2 n_2. \quad (1)$$

Here C is appropriationality constant. From the steady state condition

$$\frac{dn_2}{dt} = A_1 n_1 - A_2 n_2 = 0 \quad (2)$$

and the fact that the number of electrons in both ground and excited states added together must be equal to the total number of centers N , it follows that

$$I = \frac{A_1 A_2}{A_1 + A_2} NC. \quad (3)$$

If after steady state fluorescence is achieved, the excitation source is removed at a time taken as $t = 0$, it follows that

$$\frac{dn_2}{dt} = -A_2 n_2. \quad (4)$$

Solving for n_2 one has

$$n_2 = n_2^0 \exp(-A_2 t) \quad (5)$$

and the luminescence decays with time according to

$$I = I_0 \exp(-A_2 t) . \quad (6)$$

The major factors affecting A_1 and A_2 are the atomic selection rules perturbed by the crystal field of the center. In this model A_1 and A_2 are little affected by temperature. This type of afterglow is called spontaneous phosphorescence by Williams and Eyring⁵⁶ or fluorescence according to Kroeger²⁸, Pringsheim²⁹, and Curie³⁰.

Besides the transition $C \rightarrow D \rightarrow A$ there is a competing radiationless transition that can occur if phonons succeed in bringing the center to energy state E. In this case phonon emission of energy $E_E - E_A$ is highly probable. Such a process then can account for decreasing luminescence efficiency with increasing temperature. Luminescence efficiency is defined by Mott and Gurney⁵⁷ for steady state luminescence as being proportional to the ratio of the transition probability for radiative transition to the sum of the probabilities for all mechanisms of decay. This decrease in luminescence efficiency has been observed and reported in several cases^{58,59}.

Figure 2 presents another aspect of luminescence decay from the viewpoint of the configuration coordinate model. Supposing an electron is excited from the ground state at 1A into the higher excited state at 3B. Also suppose that the selection rules permit the transitions $3 \rightarrow 2$ and $3 \rightarrow 1$ but disallow the $2 \rightarrow 1$ transition. After sufficient excitation state 2 will become densely populated and its rate of emptying will be much slower than that of state 3 subsequent to the removal of the excitation source. Since the depopulation of state 2 depends primarily upon the thermal excitation of its electrons back to state 3 and the

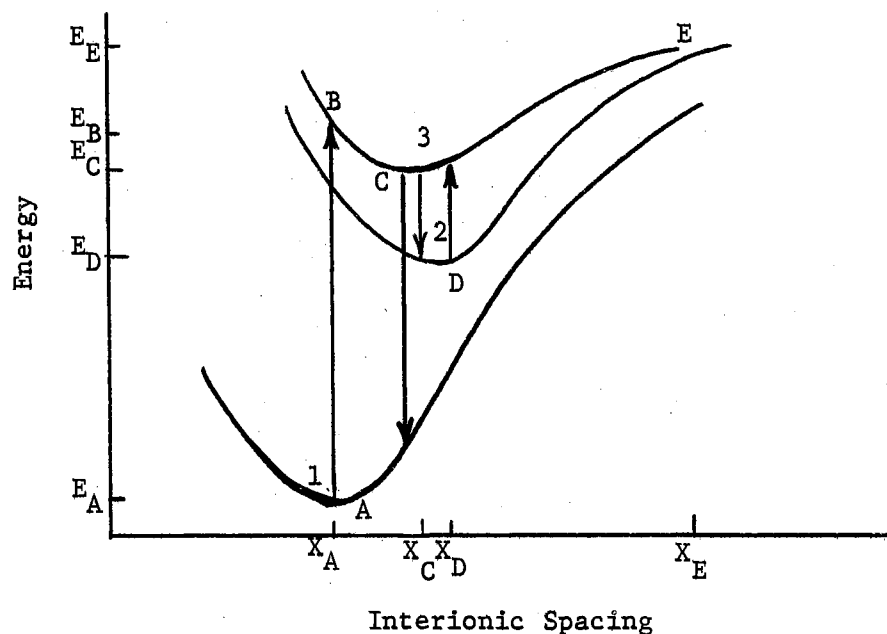


Figure 2. Configuration Coordinate Energy Level Diagram (Type II)

temperature dependence of this transition probability is proportional to $\exp \left[\frac{E_D - E_E}{KT} \right]$, the period of afterglow will increase with decreasing temperature.

The pertinent characteristics to be associated with these two cases can be summarized as follows:

Type I (Model of Figure 1):

1. Period of luminescence decay is temperature independent.
2. The form of the luminescence decay curve is independent of excitation time and intensity.
3. Luminescence decay is exponential and very rapid (decay period is about 10^{-8} second).
4. No electrical conductivity changes occur during the cycle.
5. All rate processes involve only monomolecular mechanisms.

Type II (Model of Figure 2):

1. Luminescence decay is strongly temperature dependent.
2. Luminescence is dependent upon excitation time and intensity.
3. Luminescence decay is not related to time by a simple exponential factor.
4. No electrical conductivity changes occur during the cycle.
5. Luminescence emission spectra are more characteristic of the impurity element than the host material.
6. All rate processes involve only monomolecular mechanisms.

Band Model

Although it would be desirable to describe the band model for luminescence in detail by use of a complete crystalline energy band diagram, this can not be done at present for stannic oxide because of inadequate knowledge of its band structure. Therefore, a standard flat-band picture will now be used to show how the band model can account for certain types of luminescence in a manner relevant to the present study.

Figure 3 illustrates a simplified flat-band energy level diagram with an electron trap and a recombination energy level. Here the basic

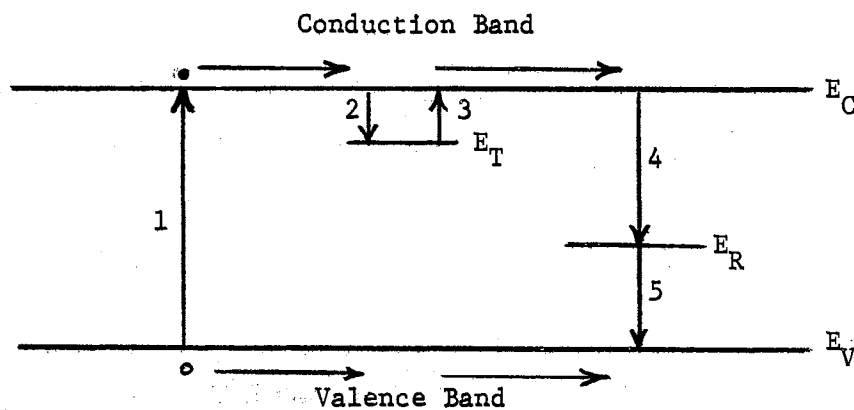


Figure 3. Simplified Energy Level Diagram for the Band Model.

luminescence cycle is shown by the following transitions:

- 1) optical excitation of valence band electrons into the conduction band,
- 2) trapping of conduction band electrons,
- 3) thermal excitation of trapped electrons back into the conduction band,
- 4) capture of conduction band electrons by a recombination center accompanied by T.S.L. emission,
- 5) recombination of electrons with holes in the valence band.

By including transitions between other levels such as $E_T \rightarrow E_V$, this model may be extended to give an explanation for phosphorescence decay of T.S.L. glow peaks when the phosphorescence is of a different wavelength than the T.S.L. glow. If transitions from E_T to E_R are permitted, then luminescence emission unaccompanied by electrical conductivity changes could be explained. Edge emission is accounted for by the transition $E_C \rightarrow E_V$.

It is because of the two distinct transitions 3 and 4 that T.S.L. measurements can be useful in the study of imperfection energy states. By analyzing the shape of the T.S.L. glow curves, the trap activation energy ($E_C - E_T$) could be determined. Also the energy location of the recombination centers could be found from a spectral analysis of the luminescence radiation. Thus for those materials whose luminescence may be described in terms of a more complicated model having the basic features of Figure 3, T.S.L. measurements should give important information about some of its imperfection energy states.

If the carrier lifetime does not change rapidly with sample tem-

perature and if there is essentially only one major recombination path, it is to be expected that the T.S.C. and T.S.L. curves should be very similar. A further discussion of the relation between T.S.L. and T.S.C. measurements is presented in the final section of this chapter.

Imperfection Centers

As the study of luminescent materials developed it was found that the luminescence efficiency in many cases could be greatly increased by the incorporation of certain impurities. Consequently these additives became known as "activators". It was also found that with the incorporation of a properly selected additional impurity it was possible to further enhance the crystal's luminescence intensity. This second added impurity was called a "coactivator" and its role has been described as that of stabilizing larger quantities of the activator element than could be maintained in the absence of the coactivator⁶⁰. An alternate explanation has been proposed that luminescent transitions occur from an excited state of the coactivator to the ground state of the activator in an associated pair⁶¹. Some materials can produce luminescence independently of the impurity concentration. These are referred to as "self-activated phosphors" and their luminescence is attributed to the presence of intrinsic imperfections such as vacancies, interstitials, microcracks, grain boundaries and stacking faults. There are also some impurity elements that will decrease the luminescence efficiency. These are referred to as "killer elements"⁶². Whether a given element will enhance luminescence efficiency or not depends upon both its nature and that of the host material.

The present state of knowledge of how the energy levels of an im-

purity and host material will interact to make possible radiative and nonradiative electron transitions is too limited to permit either a prediction of what particular combination of imperfection and host materials will increase luminescence efficiency or a prediction of the frequency of the emitted radiation. Progress in this area now comes from investigating the nature of incorporated imperfection centers in a given crystalline material and determining where their associated energy levels lie in the energy gap. The term "center" as used here will refer to that part of the surrounding crystalline structure which is appreciably distorted, as well as to the impurity ion, vacancy, etc., which is responsible for the distortion. For an impurity element the distance to which this distortion extends into the surrounding crystal depends upon its size, charge and location in addition to the polarizability of the host material. The following is a survey of some of the more common types of imperfections that are expected to affect the T.S.L. and T.S.C. processes occurring in stannic oxide.

Vacancies

Heat treatment studies of stannic oxide¹⁵ and the similarly structured material titanium dioxide⁶³ lead to the conclusion that anion vacancies predominate in these materials, giving rise to donor levels. For the purpose of the following argument an oxygen vacancy may be thought of as being created by the removal of an O^{-2} ion from the interior of the crystal to the surface. This would leave a void region having a net charge in the neighborhood of the vacancy of 2 electronic charges. The surrounding Sn^{+4} ions are repelled and the O^{-2} ions are attracted toward this vacancy. Should an electron in the conduction

band come near enough to this center it could be trapped and reduce the charge of the center to +1. Now it would be possible for either a hole or another electron to be trapped at the center. In view of the center's coulombic repulsion of holes and attraction of electrons, it seems that additional electron trapping is more likely. With a second trapped electron the center will have a neutral charge and recombination of one of the trapped electrons with a hole from the valence band is now possible. The interesting thing to note here is that it is the charge on the center that determines the capture cross section for a given type of carrier and consequently its behavior as a trapping or recombination center. Figure 4 illustrates an appropriate ordering of energy levels for the various states of ionization of an O^{-2} vacancy.

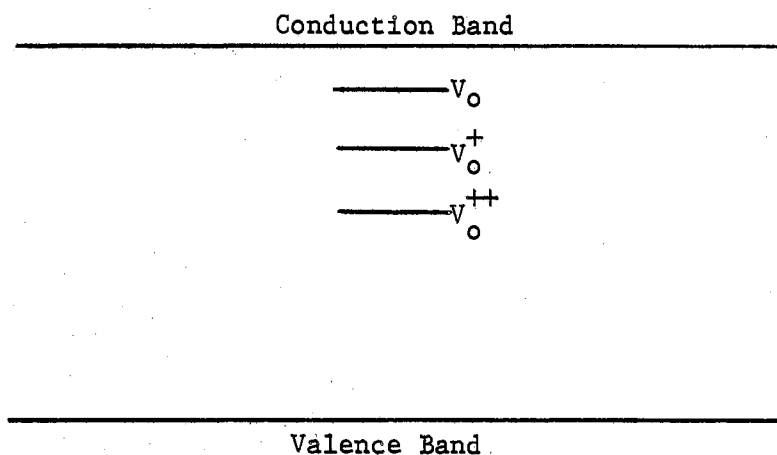


Figure 4. Energy Levels of an Anion Vacancy in Different States of Ionization

Interstitial Defects

In stannic oxide there are two likely locations at which interstitial impurity or host ions might be located. They could be in a site that had 3 tin and 4 oxygen ions as the nearest neighbors (tetrahedral

site) or in a site which had 6 oxygen ions as nearest neighbors (octahedral site). With cation interstitials the latter site seems more preferable. This is supported by the results of defect structure studies of titanium dioxide wherein it was shown that the most likely site for titanium interstitials was in the octahedral position⁶⁴. Oxygen interstitials are considered very improbable due to their relatively large size.

A neutral tin atom in an interstitial location should act as a donor imperfection because its valence electrons have energy states very close to those of the valence electrons of lattice site tin. Other metal impurity atoms will also act principally as donors depending upon their state of ionization.

Substitutional Defects

Substitutional defects are defined as impurity elements assuming the position of a host element at one of the lattice sites. The impurity differs from the host element in several ways: size, charge, directional bonding characteristics, and deformability. Each of these factors play a part in determining to what degree the surrounding crystalline structure is distorted and electronic energy levels are perturbed. As the incompatibility of impurity and host elements increase, the probability of the impurity being incorporated into an interstitial rather than a substitutional site increases. For oxides the relative ion size and valencies seem to be the major factors affecting the ability of an impurity to assume a substitutional position⁶⁵.

One way of discussing how a substitutional impurity creates energy levels lying in the forbidden gap is to treat the problem as one of

raising energy states up out of the valence band or lowering them out of the conduction band. For example, if a group IIB ion such as Zn^{+2} replaces a Sn^{+4} ion substitutionally there will be two electrons lacking in the electron exchange that normally takes place between tin and oxygen ions in stannic oxide. However, if these two electrons are made up for by two excess electrons from elsewhere in the crystal, they will have to go into orbitals of the neighboring oxygen atoms that see a different localized crystal field than would exist if Sn^{+4} were present. To indicate the fact that the substitutional ion is responsible for this raising of electron energy states of the oxygen from the valence band, Kroeger and Dikhoff⁵⁵ have adopted the notation $O^{-2}(Zn^{+2})$. In like manner a Cl^{-} substitutional for an O^{-2} ion would be expected to produce a donor level. It would be represented as $Sn^{+4}(Cl^{-})$, i.e., an energy state in the conduction band is perturbed to a lower energy state by the substitution of a Cl^{-} ion for an O^{-2} ion. Figure 5 shows types of energy levels that might be expected for different substitutionals.

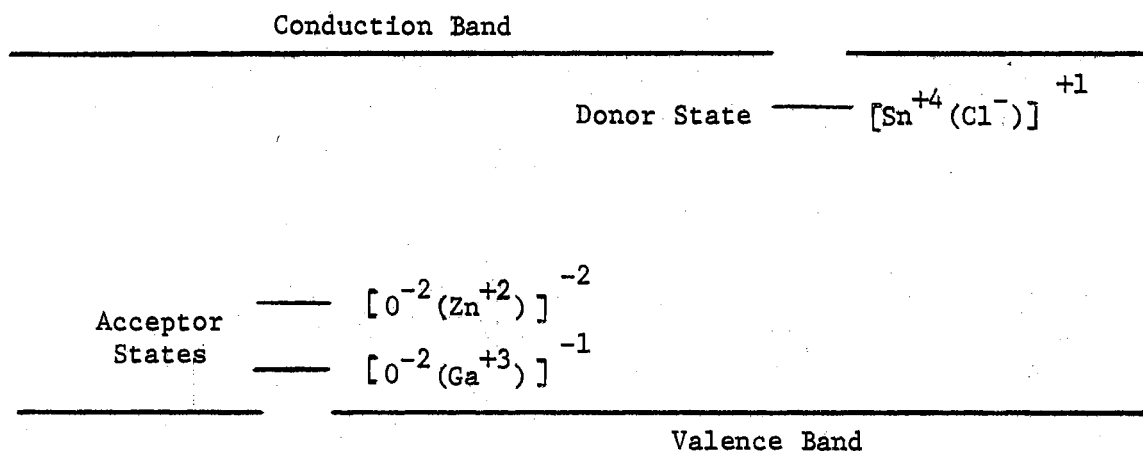


Figure 5. Acceptor and Donor Centers for Various Substitutionals in Stannic Oxide

The superscript outside the brackets give the net charge of the center after excess electron transfer has occurred. It is of interest to note that acceptor centers such as $O^{-2}(Zn^2)$ can exist in three different states of ionization. This would imply that an $[O^{-2}(Zn^+)]^{-1}$ center can capture either a hole or an electron. This type of site is not simple to consider for there are two competing factors affecting its ability to gain another electron. The fact that it already has one excess electronic charge would create a coulombic barrier that tends to exclude additional electrons, yet if an electron could be captured in the complete orbital about one of the oxygen ions the center might have a lower total energy. The variation in the degree of ionization in such centers is one of the major factors in determining their capture cross sections. At present very little is known about how to predict the properties of these multi-valent centers.

Self-Trapping

In polar crystals there is the possibility of an electron polarizing its surroundings and creating a potential well in which it can become trapped. This is to be expected at low temperatures should an electron in the conduction band remain for approximately 10^{-12} second or longer in the neighborhood of a lattice ion. Markham and Seitz⁶⁶ have made calculations for the activation energy of self-trapped electrons in NaCl and LiF and have obtained theoretical values of 0.13 eV and 0.3 eV respectively. Subsequent analysis of T.S.L. measurements by Ghormley and Levy⁶⁷ gave values of 0.14 eV and 0.32 eV respectively for the same two materials. As the covalent character of crystalline bonding increases, it would be expected that the polarizability would decrease.

In the case of titanium dioxide, which is believed to have intermediate ionic character^{68,69} similar to stannic oxide, Frederikse, et. al.⁷⁰ found the activation energy for self-trapped electrons to be about 0.01 eV at 5°K rising to 0.07 eV as the temperature increased.

Surface Traps

The energy states considered thus far have been those which can introduce defects throughout the bulk of the specimen. Due to the adsorption of ambient gases it becomes possible for additional defect energy states to exist at the surface of the crystal. An extensive amount of work has been done in the study of chemisorption involving a variety of gases and crystalline materials^{71,72,73}. In this section only the adsorption of oxygen on metal oxides will be considered.

It appears that oxygen can exist on the surface of a crystal either as physically or chemically adsorbed oxygen⁷⁴. There are three species of chemisorbed oxygen that seem likely. These are O^- , O^{-2} and O_2^- .

Matthews¹⁸ has compared the heats of formation of these three species on stannic oxide and concluded that the O_2^- species is most likely to occur. It is well known that the amount of physically adsorbed gas increases as sample temperature decreases and ambient pressure increases. In view of this it would appear that the process of chemisorption is as follows. If the surface of an initially clean metal oxide is exposed to an atmosphere of oxygen, an equilibrium concentration of physically adsorbed oxygen gas molecules will eventually be established. If the crystal is then excited by appropriate U.V. radiation, a relatively large number of electrons may be mobilized in the conduction band. The physically adsorbed O_2 molecules provide acceptor states at

the surface which act as electron traps and/or recombination centers. If Matthews' choice is correct, upon accepting an electron the oxygen molecule becomes O_2^- and is now said to be chemisorbed. If the O_2^- behaves more as a trap than as a recombination center, a charge layer will build up on the surface, creating a barrier layer for the repulsion of electrons. Figure 6 is descriptive of this process. The model has been used with success by Melnick⁷⁵ and subsequent workers to indicate the effect of oxygen on the conductance of zinc oxide. More recently, Matthews and Kohnke⁸ have extended it and applied it to polycrystalline stannic oxide.

Attempt - to - Escape Frequency

In the study of thermal excitation processes from intraband energy levels into the conduction band it is necessary to have an expression for the rate at which electrons become thermally untrapped. It has been shown from several theoretical investigations that this rate process has the general form of

$$\beta = s(E,T) \exp(-E/kT) \quad (7)$$

for both covalent⁷⁶⁻⁷⁹ and ionic materials^{80,81}. Here E is the activation energy of the trap, T is the absolute temperature and $s(E,T)$ is the so-called "attempt-to-escape frequency". Actually β is the probability of the electron escaping from the trap per unit time. For the sake of understanding the factors that affect this term a brief derivation of equation (7) is given here. A good review of this subject is given by Curie and Curie⁸².

Consider a phonon of wave vector \vec{k} moving through a crystal lattice.

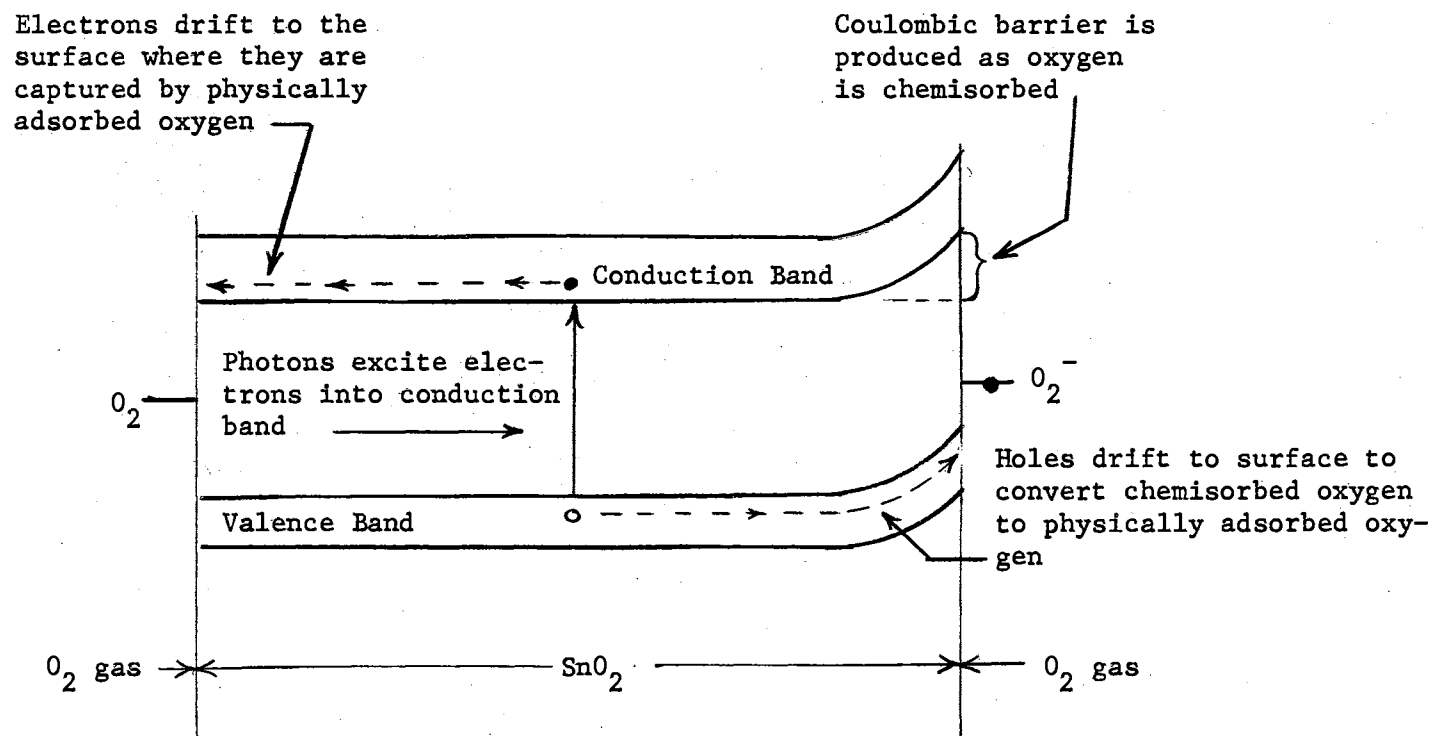


Figure 6. Model for Oxygen Gas Adsorbed on Stannic Oxide

This phonon causes the lattice ions to vibrate, which in turn introduces localized perturbations of the electric potential. The ionic displacement due to the passing of the phonon may be expressed by

$$\vec{R} = a\vec{e} \exp(2\pi i\vec{k}\cdot\vec{r}) \quad (8)$$

where the amplitude "a" of vibration is given by

$$a = \sqrt{\frac{n_k \hbar}{4\pi M \nu}} \quad (9)$$

Here \vec{e} is a unit vector in the direction of displacement, n_k is the Bose-Einstein distribution function

$$n_k = \left[\exp(h\nu/kT) - 1 \right]^{-1}, \quad (10)$$

M is the mass of the displaced ion and ν is the frequency of the phonon with wave vector \vec{k} . If $h\nu$ is greater than or equal to the activation energy E, it is possible for the phonon to untrap the electron. Assuming $h\nu = E \gg kT$, equation (10) may be approximated as

$$n_k = \exp(-E/kT) \quad (11)$$

What is more likely than a single phonon inducing the untrapping, however, is that multiphonon excitation occurs. This case has been considered by Kubo⁷⁹.

To a first approximation, the variation in the localized potential due to ionic displacement by phonons is given by

$$\delta V = -\vec{R}(\vec{r}) \cdot \text{grad } V(\vec{r}) \quad (12)$$

From quantum mechanical considerations, the transition probability per

unit time is

$$\beta = \frac{4\pi}{\hbar^2} \left| \int \psi_f^* \delta V \psi_i d\tau \right|^2 \frac{v^2}{v^3} \mathcal{V} \quad (13)$$

where ψ_f^* is the complex conjugate of the conduction band electron wave function, ψ_i is the wave function of the trapped electron, \vec{v} is the velocity of an elastic wave and \mathcal{V} is the volume of the crystal. Substitution from equations (8), (9), (11) and (12) into (13) yields

$$\beta = \frac{2\pi E \mathcal{V}}{\hbar^2 v^3 M} \left| \int \psi_f^* \left[\vec{e} \exp(2\pi i \vec{k} \cdot \vec{r}) \cdot \text{grad } V \right] \psi_i d\tau \right|^2 e^{-E/kT} \quad (14)$$

Referring to equation (14), all terms except the exponential $\exp(-E/kT)$ are usually grouped together as the attempt-to-escape frequency. It is apparent from this derivation that the attempt-to-escape frequency is dependent among other things upon charge distribution, mass, bonding characteristics, activation energy, and temperature. An adequate theory has yet to be developed which will permit a numerical evaluation of this term. At present attempt-to-escape frequencies must be determined from experimental measurements which provide only a rough order of their magnitude.

Band Models for Thermally Stimulated Luminescence

A number of variations in the band model for luminescence have been proposed over the years. One of the earlier and simpler models was proposed by Randall and Wilkins³¹ and is basically the model described earlier in Figure 3. Retrapping was considered to be negligible during this initial development but was included in a later analysis made by

Garlick and Gibson⁴¹. A further extension of this model was made by Schon⁴⁸ who included the possibility of hole transitions between the valence band and impurity energy levels.

Most materials, however, have two or more glow peaks which often are overlapping or have what appear to be broad glow peaks which may indicate nondiscrete activation energies. Broser and Broser-Warminsky⁴⁶ have investigated the theoretical characteristics of a more complex model which assumes quasi-continuous impurity level distributions. By assuming the trap density distribution did not change very rapidly over the range of energy considered they developed further expressions for the thermally stimulated current and luminescence.

For analysis of the T.S.L. and T.S.C. observed in stannic oxide, a model similar to that of Figure 7 is proposed. Using this model mathematical expressions will be developed which will ultimately lead to methods for evaluating the activation energies of electron traps in stannic oxide specimens studied.

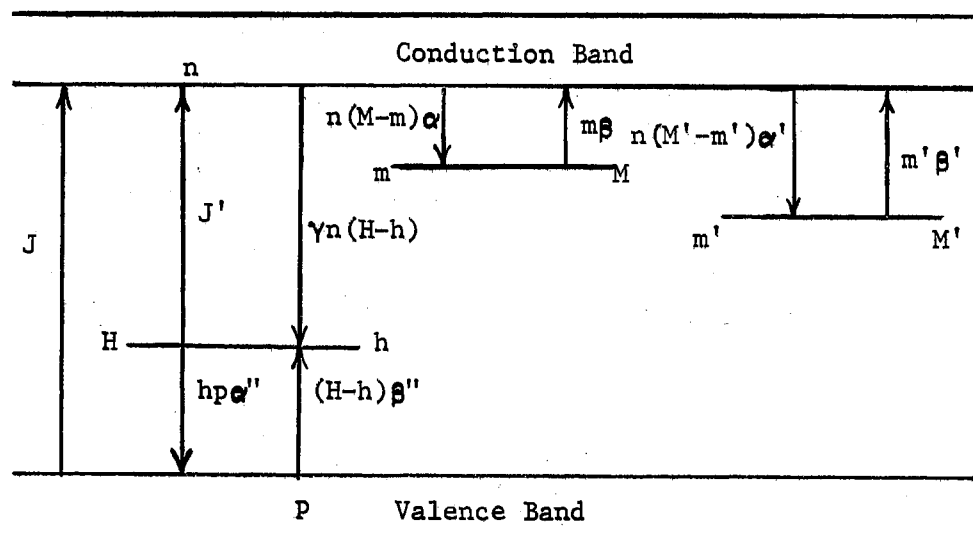


Figure 7. Energy Band Model with One Recombination Level and Two Electron Trapping Levels

The symbols in Figure 7 are defined as follows:

- J and J' - Number of electrons excited into conduction band per unit volume per unit time by incident radiation.
- H - Total density of recombination centers.
- h - Density of recombination centers occupied by electrons.
- M^i - Density of traps of activation energy E^i .
- m^i - Density of traps of activation energy E^i which are occupied by electrons.
- α^i - Transition probabilities per unit time between the indicated levels.
- β^i - Transition probabilities per unit time due to thermal excitation.
- γ - Recombination probability per unit time.

The β term was discussed in the previous section and is usually expressed in the form of equation (7).

The differential equations which describe the free carrier concentrations, n and p , and the concentrations of electrons in the three imperfection energy levels as a function of time are the following:

$$\frac{dn}{dt} = J + J' + m\beta + m'\beta' - \gamma n(H - h) - n(M - m)\alpha - n(M' - m')\alpha' \quad (15)$$

$$\frac{dm}{dt} = n(M - m)\alpha - m\beta \quad (16)$$

$$\frac{dm'}{dt} = n(M' - m')\alpha' - m'\beta' \quad (17)$$

$$\frac{dp}{dt} = (H - h)\beta'' - hp\alpha' + J \quad (18)$$

$$\frac{dh}{dt} = (H - h)\beta'' + \gamma n(H - h) - J' - hp\alpha'. \quad (19)$$

The condition for charge neutrality gives a fifth equation

$$n + m + m' = p + (H - h) . \quad (20)$$

By application of simplifying assumptions, some of which involve the control of experimentally determined parameters such as illumination time, intensity, and heat-up rates, a number of mathematical expressions may be derived for the determination of trapping parameters. For example, the experimental technique of partial thermal decay wherein the sample is heated to some predetermined temperature and then quenched to liquid nitrogen temperature, permits a relatively simple means of eliminating lower temperature glow peaks so that the shape of the higher temperature glow curves may be found. Figure 15 in a later chapter illustrates this technique.

In what follows, the assumptions and techniques used in the analysis of T.S.L. and T.S.C. for stannic oxide are given priority. It is possible that equation (15) may be solved by excluding either the third or the fourth term under the following conditions: 1) By means of partial thermal decay one can often effectively empty the shallower trap while retaining most of the electrons in the deeper trap. In this case the third term may be eliminated from the equation. 2) If the glow peaks corresponding to the two traps do not overlap so far as to strongly affect the initial rise portion of the first peak then the fourth term may be neglected during the initial rise portion of the first peak. A further simplification can be made if the deeper-lying trap is saturated. This allows the 7th term of equation (15) to be eliminated because no retrapping will occur in this level. In what follows, a discussion is given of how T.S.L. data may be analyzed to determine activation energies.

Initial Rise Method

The initial rise method is one of the more simple and versatile methods for calculating the activation energies of trapping centers. Theoretically it has been found applicable for cases involving the re-trapping and nonretrapping of electrons⁴¹. This method receives its name from the particular way in which the activation energy is related to the luminescence intensity during the initial rise of glow peaks.

The derivation begins by considering the relation between the luminescence intensity and electron trapping parameters. During the initial rise of the first peak the luminescence intensity may be expressed as the product of the number of electrons per second that become untrapped and the probability that once untrapped they will recombine with a hole trapped at a recombination center. It is assumed that there is negligible buildup of electrons in the conduction band and that the recombination lifetime is very short. Accordingly, the luminescence intensity produced during the emptying of traps M and M' respectively may be written

$$L = C \left(\frac{m + m'}{M + M'} \right) ms \exp(-E/kT) \quad (21)$$

$$L = C \left(\frac{m'}{M + M'} \right) m's' \exp(-E'/kT) \quad (22)$$

Here C is a proportionality constant and the terms in the first parentheses are the probabilities of nonretrapping. These terms are obtained by assuming the number of empty recombination centers is equal to the number of filled traps. By taking the ratio of the density of empty recombination centers $(m + m')$ and the total density of empty centers of

all kinds, $(M - m) + (M' - m') + (m + m')$, the nonretrapping probability is obtained. For the second trap, m is considered negligible due to previous thermal quenching.

Equation (21) also makes use of the assumption discussed in the previous section concerning the separability of the initial rise portions of the glow curves. Since the luminescence intensity is determined by the rate at which conduction band electrons return to the recombination centers, we have

$$L = C \gamma n (H - h) . \quad (23)$$

Now making use of the charge neutrality condition (20) and the assumption that the build up of conduction band electrons is negligible, one obtains for the initial emptying of the first trap

$$\frac{dm}{dt} = \frac{dp}{dt} - \frac{dh}{dt} . \quad (24)$$

Substitution from equation (18) and (19) into the terms on the right side of equation (24) yields

$$\frac{dm}{dt} = -\gamma n (H - h) . \quad (25)$$

Using equations (23), (25) and (21), one has

$$\frac{dm}{dt} = - \left(\frac{m + m'}{M + M'} \right) m s \exp -E/kT . \quad (26)$$

The application of a constant heat-up rate, $dT/dt = b$, makes it possible to solve equation (26) for the density of trapped electrons as a function of temperature:

$$m = m_o \left[\left(1 + \frac{m_o}{m'}\right) \exp \left\{ \frac{m'}{M + M'} \int_{T_o}^T \frac{s}{b} e^{-E/kT} dT \right\} - \frac{m_o}{m'} \right]^{-1} \quad (27)$$

Substitution of (27) into (21) gives (28)

$$L = \frac{C m_o^2 s e^{-E/kT} \left(1 + \frac{m'}{m_o} \left[\left(1 + \frac{m_o}{m'}\right) \exp \left\{ \frac{m'}{M + M'} \int_{T_o}^T \frac{s}{b} \exp^{-E/kt} dT \right\} - \frac{m_o}{m'} \right] \right)}{(M + M') \left[\left(1 + \frac{m_o}{m'}\right) \exp \left\{ \frac{m'}{M + M'} \int_{T_o}^T \frac{s}{b} \exp^{-E/kT} dT \right\} - \frac{m_o}{m'} \right]^2}$$

Now for the initial rise portion of the first glow peak the integrals appearing in equation (28) are small. This permits equation (28) to be approximated by

$$L = C \frac{m_o^2 s \exp^{-E/kT}}{M + M'} \quad (29)$$

Upon taking the natural logarithm of equation (29) and differentiating with respect to the inverse temperature one has

$$E = -k \frac{d(\ln L)}{d(1/T)} \quad (30)$$

From equation (30) it is seen that the activation energy may be readily determined from the slope of a graph of $\ln [L(T)]$ vs $1/T$ for the initial rise portion of the first glow peak. It should be pointed out that if the activation energy E is strongly dependent upon temperature then equation (30) is not valid. In some materials the electron traps are found to be distributed over a range of energies. In such a case there is still some question as to the accuracy with which activation energies may be determined by the initial rise method.

Equation (22) is very similar to the case considered by Garlick

and Gibson⁴¹. Thus the T.S.L. for the second peak as a function of temperature may be written as

$$L(T) = \frac{C m_o'^2 s' \exp^{-E'/kT}}{(M + M') \left\{ 1 + \frac{m_o'}{M + M'} \int_{T_o}^T \frac{s'}{b} \exp^{-E'/kT} dT \right\}^2} \quad (31)$$

This leads to the same expression for the activation energy of the second peak as equation (30). A good critique of the initial rise method has been presented by Braunlich⁸³.

Statement of Other Methods

In addition to the initial rise method, there are numerous other methods which are worthy of mention. Methods based on the shape of the individual glow peaks have been utilized by several workers. The activation energy is found as a function of the temperatures corresponding to the maximum and the half-maximum luminescence intensities^{43,84-87}. Booth⁴² developed a method of calculating activation energy involving the relation between glow peak temperature and the heat up rate. This particular method is not applicable when retrapping occurs. An analysis technique employed by Kelly and Laubitz⁸⁸ made use of nonlinear heating rates. Applying heat-up rates that were proportional to the square of the absolute temperature, they found that the integrals such as those in equations (28) and (31) could be evaluated to give relatively simple expressions for the activation energy of both 1st and 2nd order processes. Among the earlier techniques devised was that of obtaining relations between the area under the glow curves and the trap activation energies. It too was applicable for both monomolecular and biomolecular

decay processes^{89,90}. There are several good reviews of the various methods of analyzing both T.S.L. and T.S.C. data^{49,87,91}.

Ultimately, simplicity of experimental arrangement and the observation of overlapping or closely-spaced glow peaks in the present work dictated the choice of the initial rise method as the most practical approach for analyzing experimental data obtained. Booth's method was also investigated but gave generally unsatisfactory results.

Correlation of T.S.L. and T.S.C.

Use is made of the assumptions given in the previous section for deriving relations between T.S.L. intensity, $L(T)$ and the T.S.C. conductivity, $\sigma(T)$. In the simplest sense which considers each glow peak and its corresponding T.S.C. maximum separately, the rate of change of electron concentration in the conduction band may be expressed as

$$\frac{dn}{dt} = \frac{-n}{\tau} - \frac{dm}{dt} \quad (32)$$

where τ is the recombination lifetime. Equation (32) is the same as equation (15) if $J = J' = \alpha' = \beta' = 0$ and $\tau = \frac{1}{\nu(H-h)}$. Substitutions from equations (23) and (25) using the assumption that the recombination lifetime is very small (this is found to be a valid assumption for most phosphors) allow equation (32) to be solved for conduction band electron concentration which is

$$n = C \tau L(T), \quad (33)$$

or in usual terms of the electrical conductivity,

$$\sigma(T) = ne\mu = Ce\mu \tau L(T) \quad (34)$$

where e is the electronic charge and μ is the mobility of conduction band electrons. From equation (34) it is seen that T.S.C. and T.S.L. peaks will not necessarily occur at the same temperatures. This is due to the possibility of a temperature dependence for the mobility and the recombination lifetime. According to Garlick and Gibson⁴¹ the T.S.C. peak may be as much as 10°C higher than the T.S.L. peak. A comparison of the T.S.C. and T.S.L. peaks in zinc sulfide indicate that in one instance the T.S.C. peak occurs at about 7°C higher temperature than the T.S.L. peak⁴⁶.

CHAPTER III

EXPERIMENTAL DETAILS

Samples

Various heat treated and doped samples of stannic oxide single crystals and ceramics were investigated for thermally stimulated luminescence. The single crystals were chosen from among those obtained from Corning Glass Works and those grown locally by Kunkle⁹². The ceramic samples were also produced locally by Matthews¹⁸.

The locally-grown single crystals were produced by a flux growth method. A mixture of two parts stannic oxide was placed with one part cuprous oxide by volume in a platinum crucible. This was heated in an electric furnace to approximately 1250°C for several days and slowly cooled to room temperature. The samples obtained from the melt were transparent colorless needles or rods with their greater dimension along the c-axis. The cross section of these needles was square in shape. Typical dimensions of sample-sized crystals grown by this process were $\frac{1}{2} \times \frac{1}{2} \times 2$ to 3 mm. Spectrographic analysis* gave impurity concentrations of 0.002% of Cu_2O and 0.02% SiO_2 by weight.

The Corning specimens were produced by a vapor transport technique⁹³. These samples were generally clear and transparent. Those

* Analysis by the Bruce Williams Laboratory, Joplin, Missouri.

actually used consisted of a long needle of dimensions 1 x 1 x 10 mm and some odd sized chunks. No impurities concentrations were given for these samples although one was believed to contain some iron. In connection with E.S.R. experiments, two of the specimens were locally diffusion-doped with copper and nickel and are so identified in Figure 17 to be presented later.

Two types of ceramic samples were prepared by Matthews by pressing and firing procedures described in his M.S. thesis⁹⁴. These were pure and zinc-doped ceramic pellets. The zinc-doped samples were prepared from mixtures containing 0.7% and 10% zinc oxide by weight. In general the samples were prepared by pressing the powders to 10,000 psi and firing in air at about 1400°C for periods of time varying from 4 to 100 hours. The grain size was about 5 microns. The pellets were very hard, white in color and were above 90% crystalline density.

The pure stannic oxide pellets were pressed from reagent grade stannic oxide powder and fired in a manner similar to that of the zinc-doped samples. The grain size of these samples which were also white in color was found to be about 4 to 5 microns. For both the doped and pure ceramics, the final samples were cut from the center of the original $\frac{1}{2}$ inch diameter pellets. The dimensions of the specimens were 3 x 3 x 2 mm. Electrical properties of specimens of this type have been discussed in some detail by Matthews¹⁸.

Apparatus

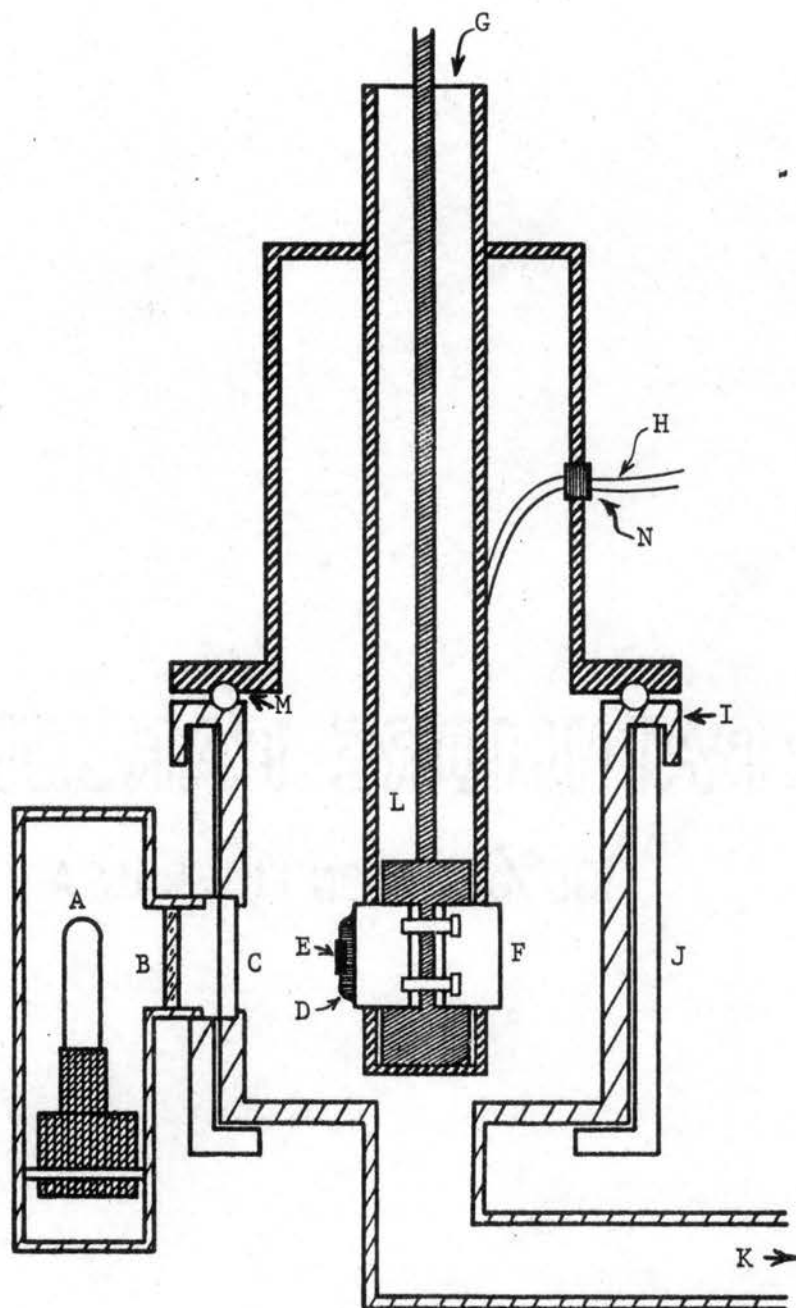
The basic components of the apparatus for making T.S.L. measurements consist of a sample heating and cooling system, a vacuum system, a luminescence detection device, apparatus for monitoring the sample

temperature, and a UV light source. Figure 8 shows how these various components were arranged with respect to one another. The inner vacuum can I was held stationary while an outer light can J supporting the light source A and the photomultiplier tube assembly was free to rotate. This design permitted the irradiation of the samples E at near liquid nitrogen temperatures under 10^{-2} torr pressure. After irradiation the light can could be rotated through 120° to bring the photomultiplier tube into place facing the sample. A quartz window C was mounted in the vacuum can to permit the passage of light to and from the sample. The details concerning the basic components of the apparatus are as follows:

Sample Heating and Cooling System

In order to control the sample temperature as uniformly as possible, the samples were imbedded in a pool of molten indium D deposited on the copper sample mount F. The sample mount in turn was attached to the stainless steel cryostat G. A strip of tin foil containing a hole the same size as the sample was next wrapped around the sample mount and cryostat to serve as a thermal shield. It was found that this permitted the sample temperature to be lowered an additional 15 to 20°C to a value as low as -196°C . It also reduced background luminescence to a negligible factor. The sample heat-up rates were regulated by a 100 watt electrical heating element L that could be inserted into the nitrogen well. Nearly linear heat-up rates were obtained by manually controlling the heater voltage with a variable voltage transformer. Over the region of the initial rise of a glow peak the variation of heat-up rates could be held to less than 5%.

Sample Temperature Monitor



- | | |
|-------------------------|----------------------------------|
| A. Mercury Lamp | H. Thermocouple Leads |
| B. 3130 Å Filter | I. Vacuum Can |
| C. Quartz Window | J. Light Can |
| D. Indium Sample Holder | K. Cold Trap and Mechanical Pump |
| E. Sample | L. Heating Element |
| F. Copper Sample Mount | M. O-Ring Seal |
| G. Liquid Nitrogen Well | N. Quartz Feed Through |

Figure 8. T.S.L. Apparatus

Thermocouple leads H were wrapped several times around the liquid nitrogen well so that heat leaks to the sample would be decreased. The problem of making good thermal contact between thermocouple and sample was eliminated by immersing the thermocouple junction next to the sample in the indium melt. The sample itself was immersed to its upper surface in order to achieve a more uniform temperature. The thermocouple voltage was recorded by a model SR Sargent strip chart recorder. The recorder was calibrated by comparison with a Leeds-Northrup K3 potentiometer. Standard copper-constantan calibration was used for temperature determination.

Vacuum System

A mechanical forepump and a liquid nitrogen cold trap were used to obtain a vacuum of the order of 10^{-3} Torr.

Luminescence Detector

A 1P-28 photomultiplier tube was used to detect the sample luminescence. Its effective range of spectral sensitivity extends from 2200 to 6000 Å°. The operational voltage of the tube was limited to about 850 volts. Above this value discharges within the voltage divider would occur when the tube was in a vacuum for cooling purposes. The electrical circuit diagram of the tube's voltage divider is given in Figure 9. The tube current output was converted to a voltage signal by a Keithley 610-B electrometer. This voltage signal was then fed into a model SR Sargent strip chart recorder similar to the one used for monitoring sample temperatures. Both strip chart recorders were run at the same speeds so that it was possible to easily match sample temperature with

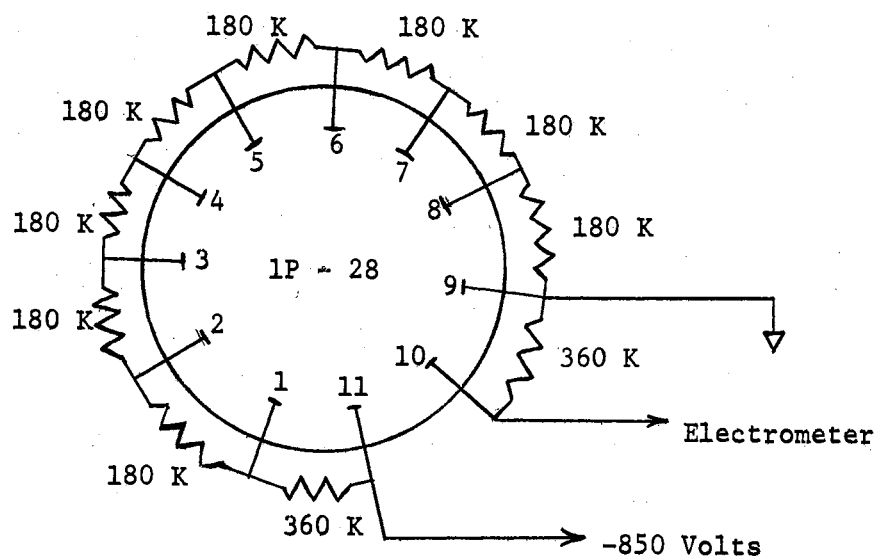


Figure 9. Circuit Diagram of Photomultiplier Tube Voltage Divider

luminescence intensity.

Figure 10 gives a block diagram of the temperature and luminescence measuring systems. By cooling the photomultiplier tube it was found that the tube's dark current could be decreased by a factor of 100 or more. Essentially the same design for the tube housing and cooling apparatus as reported by Halperin and Kristianpoller⁹⁵ was used in this instance. Figure 11 gives details of the tube cooling system. A small heating coil I was wrapped around the quartz window A in order to prevent moisture from condensing on it. A thermocouple soldered to pin 9 of the voltage divider H served not only as a ground but also as a means of measuring its temperature. It was found that the tube circuit would cool to -115°C in 1 hour when the brass rod K was immersed in liquid nitrogen. A kovar-to-pyrex glass-to-metal seal J of 1 inch O.D. was used to connect the glass shield B to the brass rod. The tube was fitted into a demountable brass cylinder F. To insure electrical and

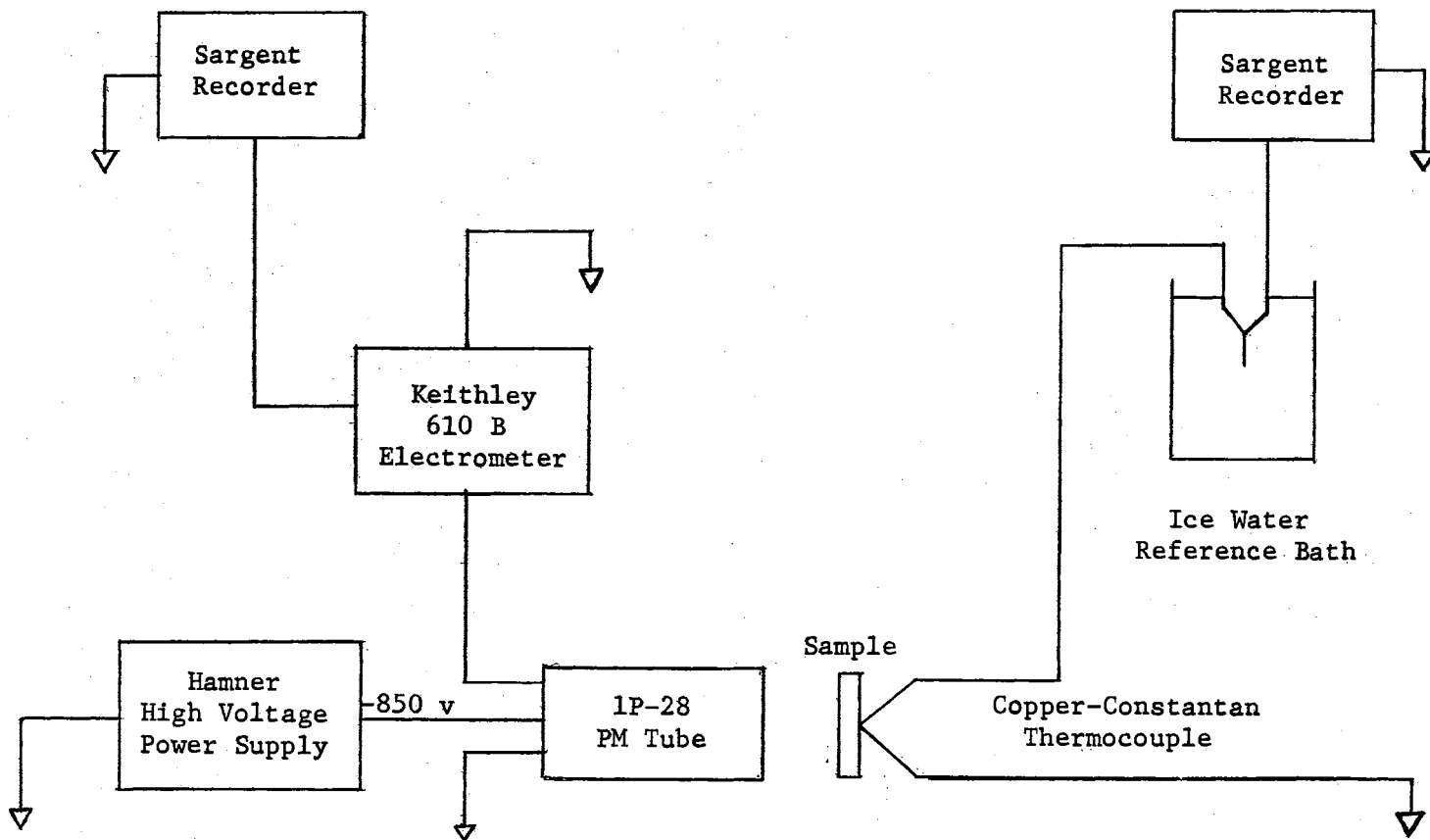


Figure 10. Block Diagram of T.S.L. Electronic System

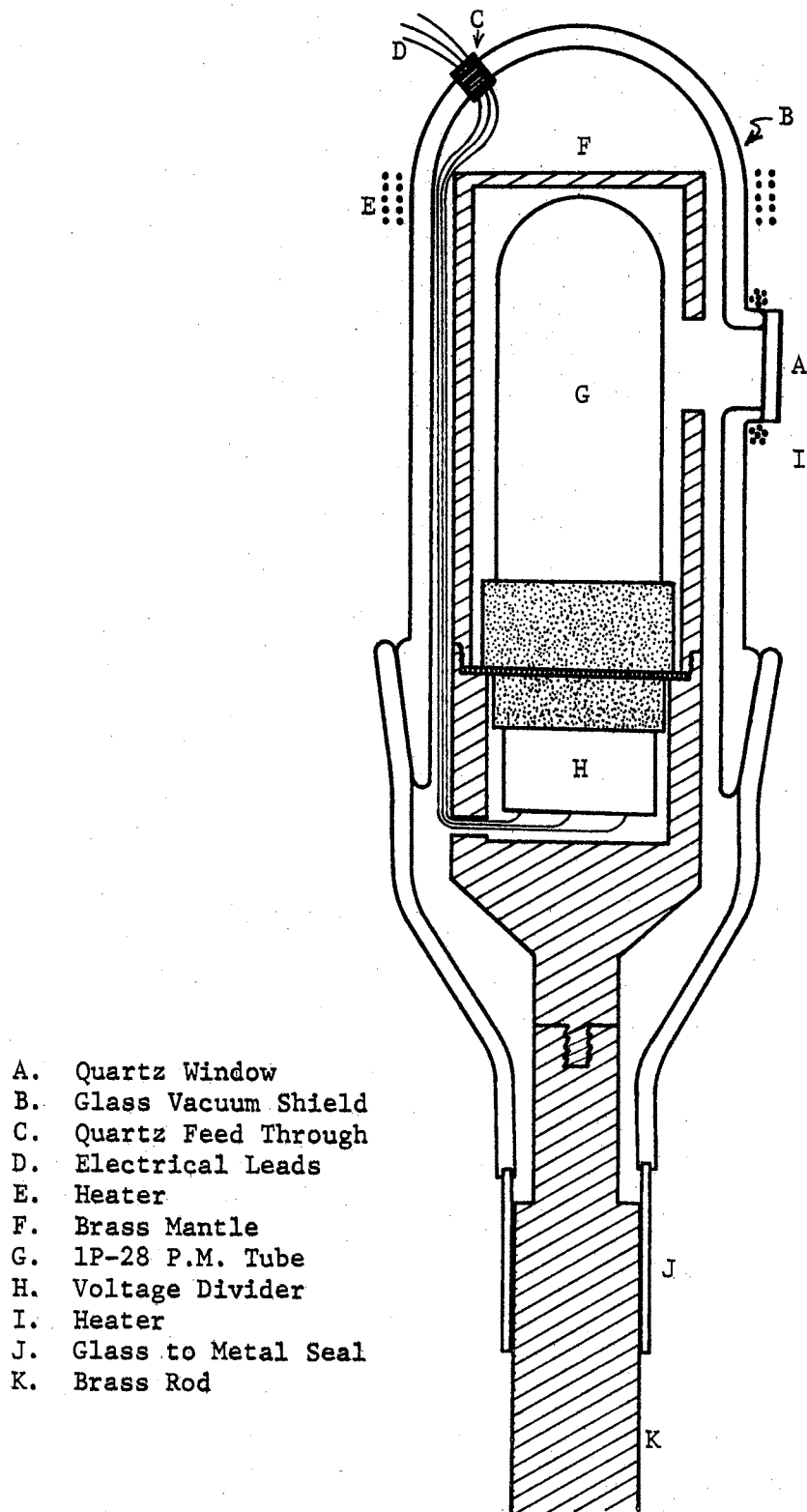


Figure 11. Photomultiplier Tube Cooling Assembly

magnetic shielding a double layer of tin was placed around the glass shield and the brass rod was also grounded. Optical shielding was obtained by painting the glass shield black and wrapping it in a layer of black felt.

Light Source

The sample was irradiated by a Hanovia type S.H. mercury lamp. Normally the irradiating light was passed through a Baird Atomic UV filter with peak transmission at 3130\AA . The band width at 50% peak transmission was 200\AA .

Experimental Techniques and Procedures

A typical T.S.L. run might be described in the following manner:

- a) the sample is mounted and is cooled to liquid nitrogen temperature while in the dark at about 10^{-3} Torr, b) it is then exposed to the excitation radiation for a predetermined length of time, c) the irradiation source is removed and the after glow is permitted to decay to an appropriate level, d) the sample is then heated at some constant rate and data taken of photomultiplier output versus thermocouple voltage. In this basic manner T.S.L. measurements were made from about -190°C to $+170^{\circ}\text{C}$. The upper limit of 170°C was imposed by the melting point of the indium sample holder.

Several extensions and modifications of the basic experiment were also used in the work reported here. Polarization and spectral output of the luminescence were studied. The effect of the wavelength of the exciting radiation was observed. Specimens were subjected to different heat treatments prior to obtaining experimental data. Partial thermal

decay measurements were carried out in an attempt to refine the calculations of activation energies. Some explicit details will now be given.

A rough spectral analysis of the T.S.L. was made by inserting a series of Baird Atomic filters between the sample and the photomultiplier tube. These filters had peak transmissions at 3130 \AA , 4000 \AA , 4600 \AA , and 5400 \AA . The 3130 \AA filter had a band width at 50% peak transmission of 200 \AA . The others were 860 \AA wide at 50% peak transmission. These same filters were used to filter the excitation radiation in order to obtain a series of T.S.L. curves for a single crystal. A Glan-Thompson calcite polarizer with spectral transmission from 3100 \AA to $23,000 \text{ \AA}$ was used to determine the direction and degree of T.S.L. polarization for directions parallel and perpendicular to the c-axis of single crystals.

The heat treatment studies consisted of heating the samples between 100°C and 170°C for 24 hours or longer in either air at atmospheric pressure or at a reduced pressure of 10^{-2} Torr. The vacuum heat treatments were made with the samples mounted on the cryostat for two reasons: a) to prevent sample exposure to the atmosphere after heat treatment and prior to T.S.L. run, and b) to insure that the geometry of the experiment remained unchanged for both air and vacuum heat treatments.

The partial thermal decay technique, as stated previously, provides a convenient method for separating glow peaks that do not excessively overlap. It was found that by using $0.1^\circ\text{C}/\text{sec}$ heat-up rates greater control could be had over the temperature at which the thermal decay was terminated. Just a few degrees below the maximum thermal decay temperature the sample would be recooled to -190°C . Then the sample could again be heated at a constant rate to obtain a new glow curve for the

higher temperature peaks. The reasons for these procedures and the extent to which they assisted in developing and analyzing a T.S.L. model for stannic oxide will become evident in the next two chapters.

The samples were prepared for T.S.L. measurements by observing the following cleaning procedure.

- a) a wash in acetone in ultrasonic cleaner
- b) a wash in methanol in ultrasonic cleaner
- c) a wash in distilled water in ultrasonic cleaner
- d) boiled for 20 min. in aqua regia
- e) rinsed in distilled water
- f) boiled 20 min. in HCl
- g) rinsed in distilled water in ultrasonic cleaner
- h) rinsed in methanol in ultrasonic cleaner
- i) heated in air at 150°C for at least 24 hours

This cleaning procedure was to insure the surfaces were free of foreign matter and dry prior to each series of T.S.L. runs.

CHAPTER IV

EXPERIMENTAL RESULTS

Introduction

In this chapter a systematic presentation of the experimental results will be given. These will be ordered in the following manner:

Basic T.S.L. Measurements

This section presents a discussion of those experimental factors such as exposure time, heat-up rate, initial decay time and partial thermal decay temperature that affect the fundamental shape of glow curve.

Analysis of T.S.L. Radiation

As indicated in the preceding chapter the T.S.L. radiation was analyzed according to its wavelength and direction of polarization. The results of such measurements are given in this section.

Excitation Radiation

The effect of irradiating the sample with various wavelength ranges of incident light is reported here.

Heat Treatment Studies

Here are given the results of heat treatment and some other observations that indicate effects of adsorbed oxygen on T.S.L.

A large number of experiments were done using a variety of controlled conditions as applied to both single crystal and ceramic specimens. Although all the results are not presented here, certain characteristic features were noted for samples of both types. This necessitates categorization of the observations both as to sample type and to the particular experiment carried out.

Basic T.S.L. Measurements

For the proper understanding and interpretation of T.S.L. data it is necessary to know some of the experimental factors that affect the shape of glow curves. In many instances the glow curves of the same sample are apparently different in structure. This may be accounted for by differences in excitation time, heat-up rate, initial decay time and maximum partial thermal decay temperature.

Excitation Time

Other than an increase in the total output light sum, the principal effect of increasing the excitation time is to cause an apparent merging of adjacent peaks and thus decrease in their resolution for a given complete glow curve. This is illustrated in Figure 12 for a locally-grown single crystal. It will be seen that for a 5 second excitation time there are at least four peaks present. As the excitation time is increased to 30 minutes three of these peaks merge to form a single peak at an intermediate temperature between the -96°C and the -125°C peaks. The "waiting time" or the initial decay time at -190°C was 15 minutes for each of the glow curves shown.

Heat-up Rate

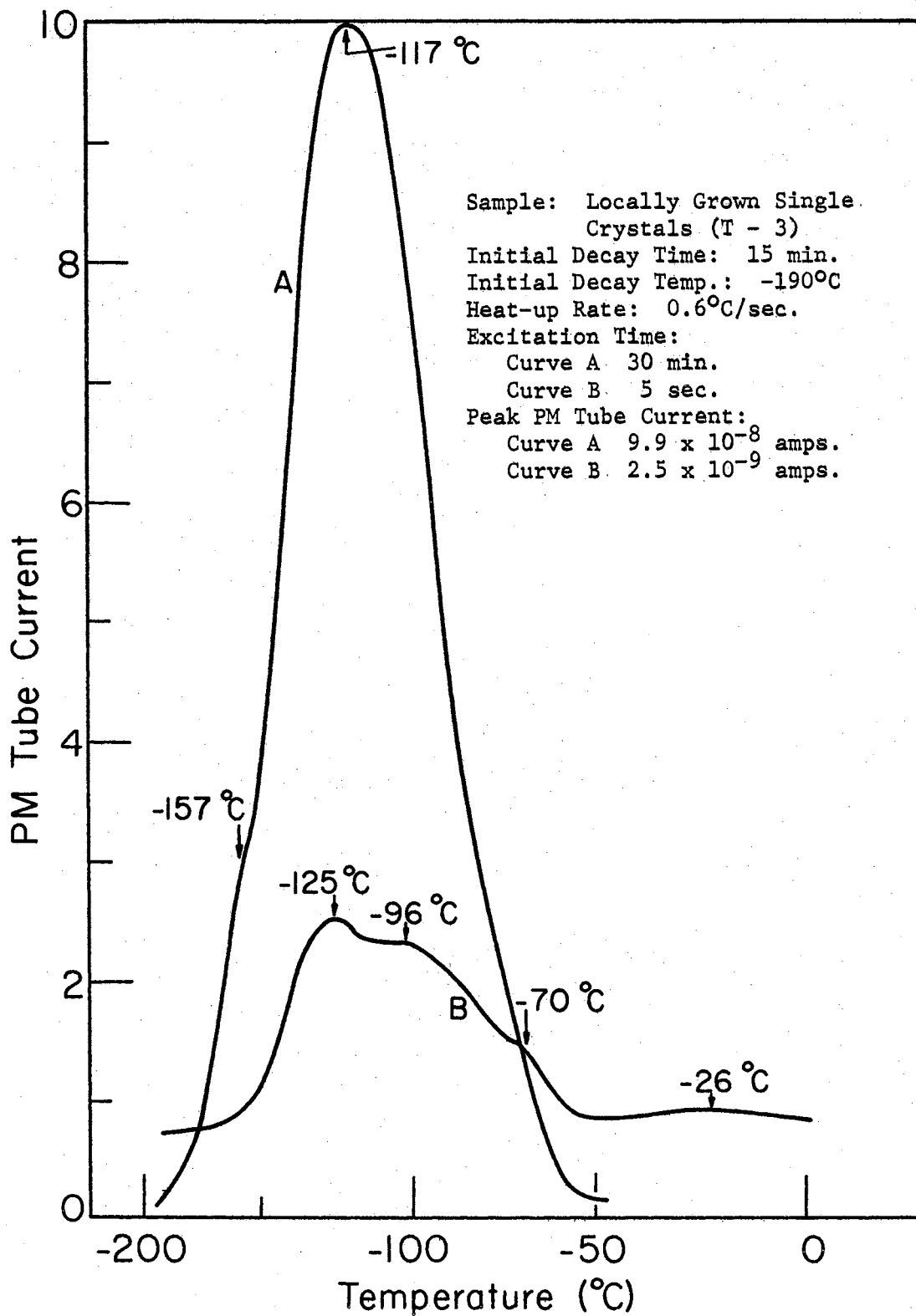


Figure 12. Effect of Excitation Time on Glow Curves.

There are two effects associated with the heat-up rate. One is to decrease the maximum luminescence intensity as the heat-up rate decreases. The second is to shift the glow peak to higher temperatures as the heat up rate increases. The first effect is to be expected since trapped electrons are being released more slowly, decreasing the number of recombination events per unit time. The second effect is common in glow curve experiments and forms a basis for Booth's method⁴¹ of calculating activation energies which was mentioned earlier. Figure 13 gives a comparison of the effect of different heat-up rates for a locally-grown single crystal.

Initial Decay Time

The initial decay time or the waiting time is the time the sample is permitted to remain at liquid nitrogen temperature prior to heat-up. An increase in the waiting time results in a partial decay of the peak at -160°C . Figure 14 illustrates the change in the glow curve as the waiting time is increased for an undoped ceramic sample. The indications are that a very prominent glow peak would occur at -160°C if the sample temperature could be further reduced during excitation.

Partial Thermal Decay Temperature

This is the maximum temperature to which a sample is raised during partial thermal decay. Such a decay in effect decreases or eliminates all the contribution to the glow curve by peaks that lie at temperatures below it. Figure 15 shows the effect of partial thermal decay in eliminating the lower temperature peaks from the glow curve of a ceramic sample.

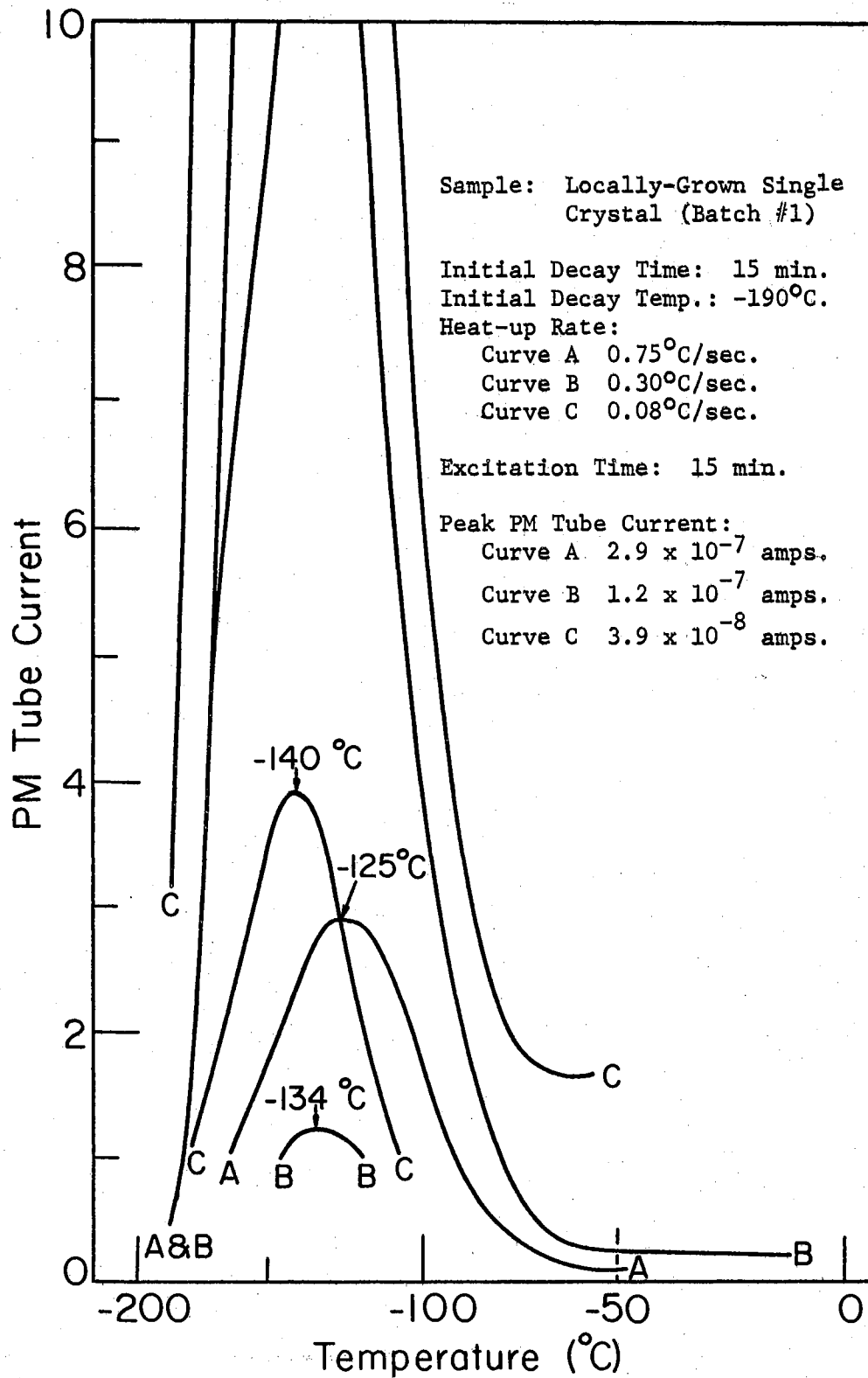


Figure 13. Effect of Heat-up Rates on Glow Curves

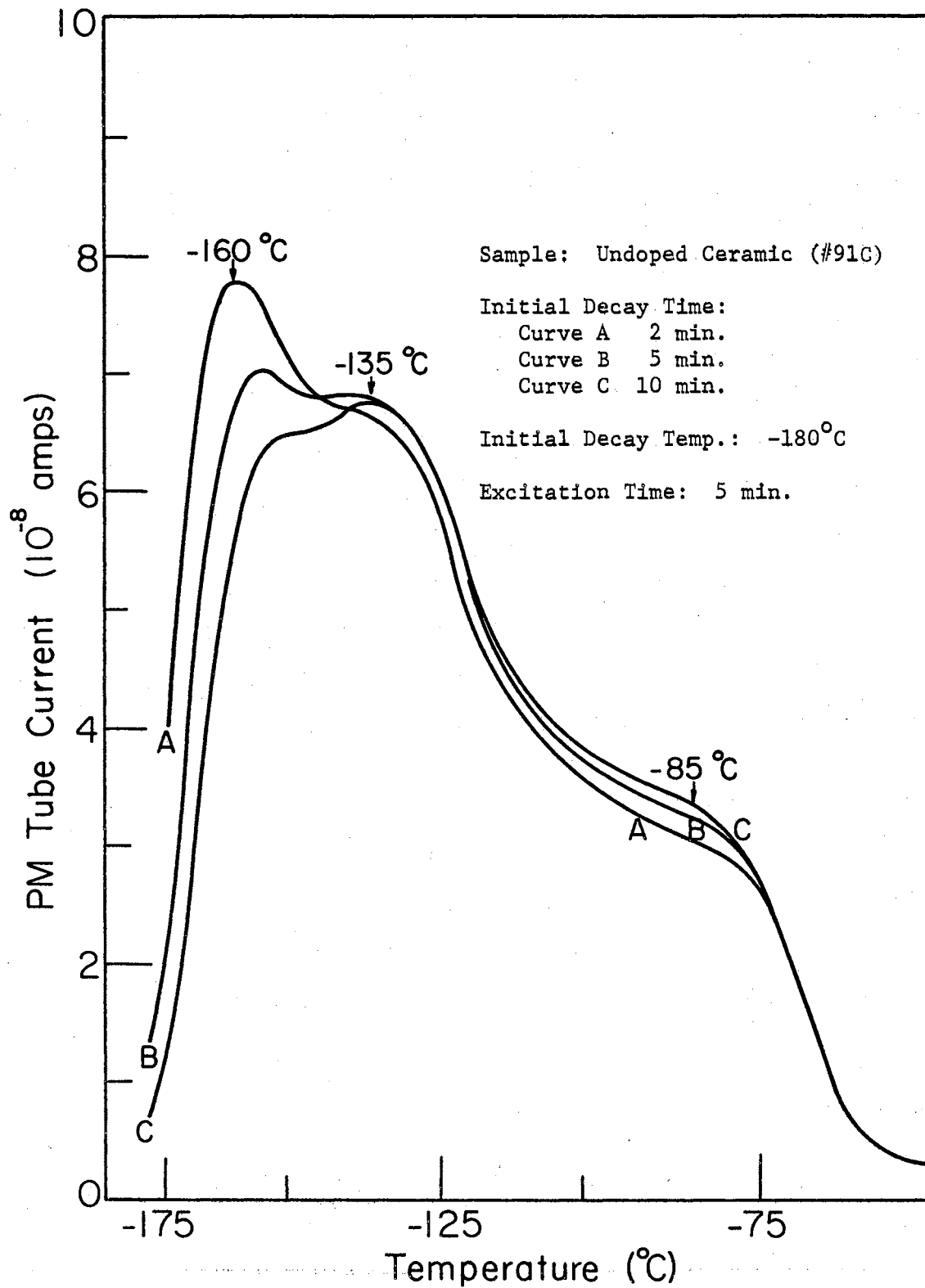


Figure 14. Effect of Initial Decay Time on Glow Curves

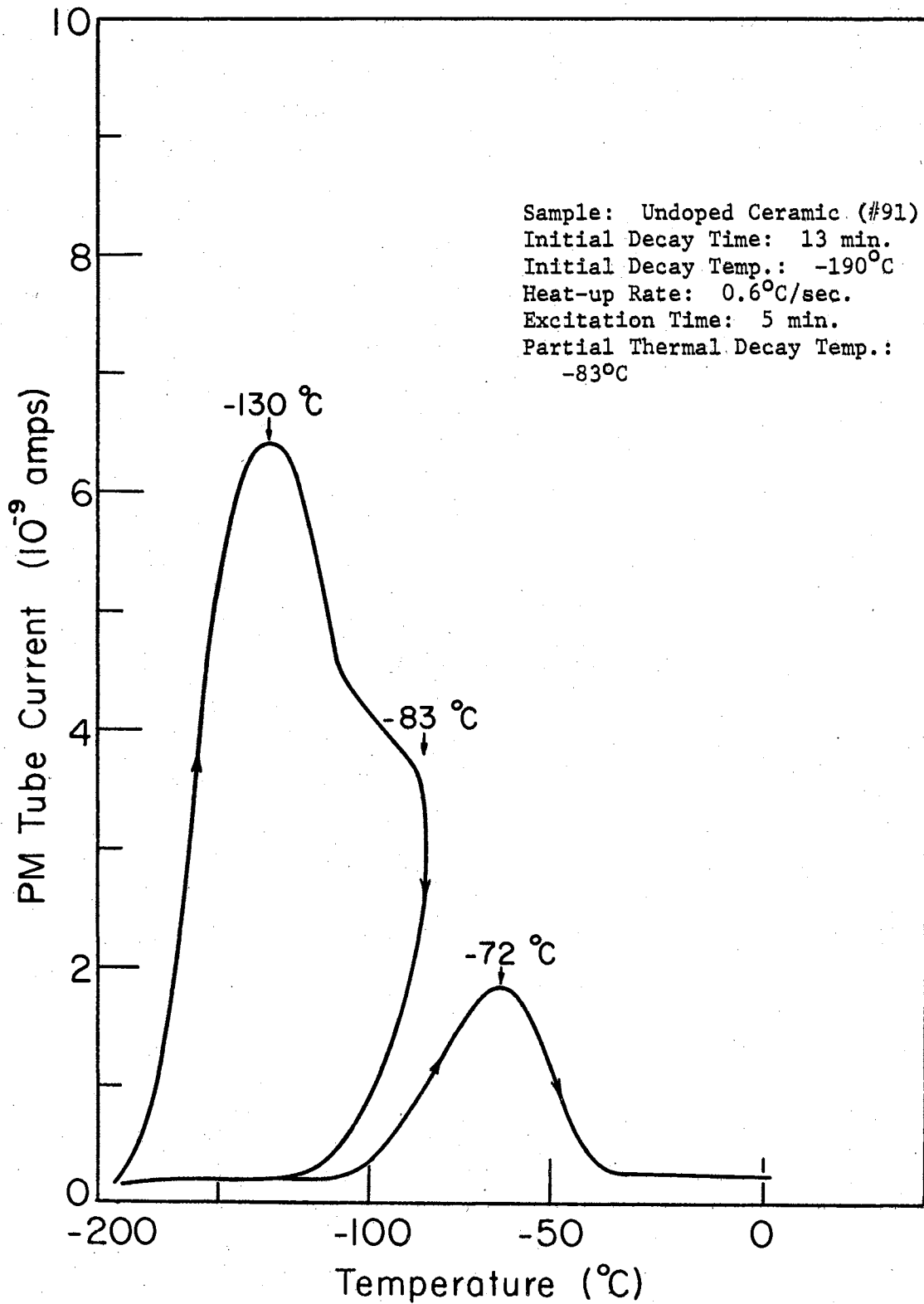


Figure 15. Effect of Partial Thermal Decay on Glow Curves

With the above facts in mind it is now appropriate to compare characteristic glow curves for various samples investigated in this study. Figures 16, 17 and 18 display the glow curves that are representative of locally-grown single crystals, Corning single crystals, and variously doped ceramics, respectively. It will be seen that there are basically five different peaks present in the single crystal samples. It is the relative luminescence intensity associated with each of these individual glow peaks that ultimately determines the gross shape of the glow curve for a given specimen. Allowing for variations in the four factors discussed above, it appears that the peak temperatures occur at about -165°C , -135°C , -90°C , -60°C , and -15°C . The data indicates that there are no peaks above -90°C in the ceramic samples although the others are present in varying degree. In several single crystals investigated it was also found that the -60°C and -15°C peaks were absent. The question to be raised is whether the defects responsible for these peaks are absent from the samples or whether the density of such defects is simply too small to give a detectable glow peak.

Analysis of T.S.L. Radiation

The luminescence radiation was analyzed as to its spectral distribution and its direction of polarization. Actually only a rough analysis of the spectral distribution was made using optical filters supplemented by visual observations. Although a complete series of curves was not run for each sample, visual observations showed that they each had the same yellowish-colored luminescence. Figure 19 shows several filtered glow curves for a locally-grown single crystal.

The polarization study was limited to detecting that light which

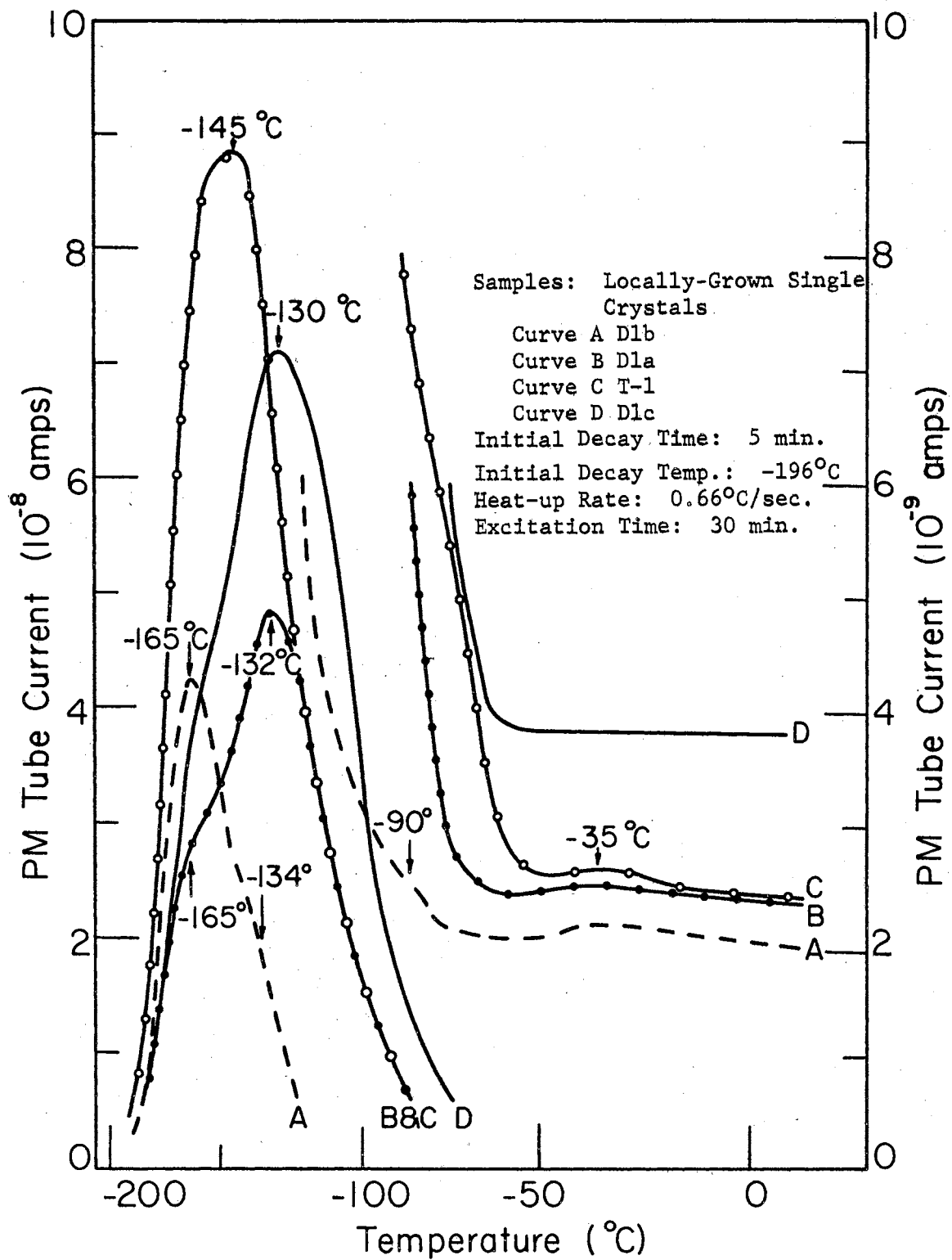


Figure 16. Representative Glow Curves of Locally-Grown Single Crystals

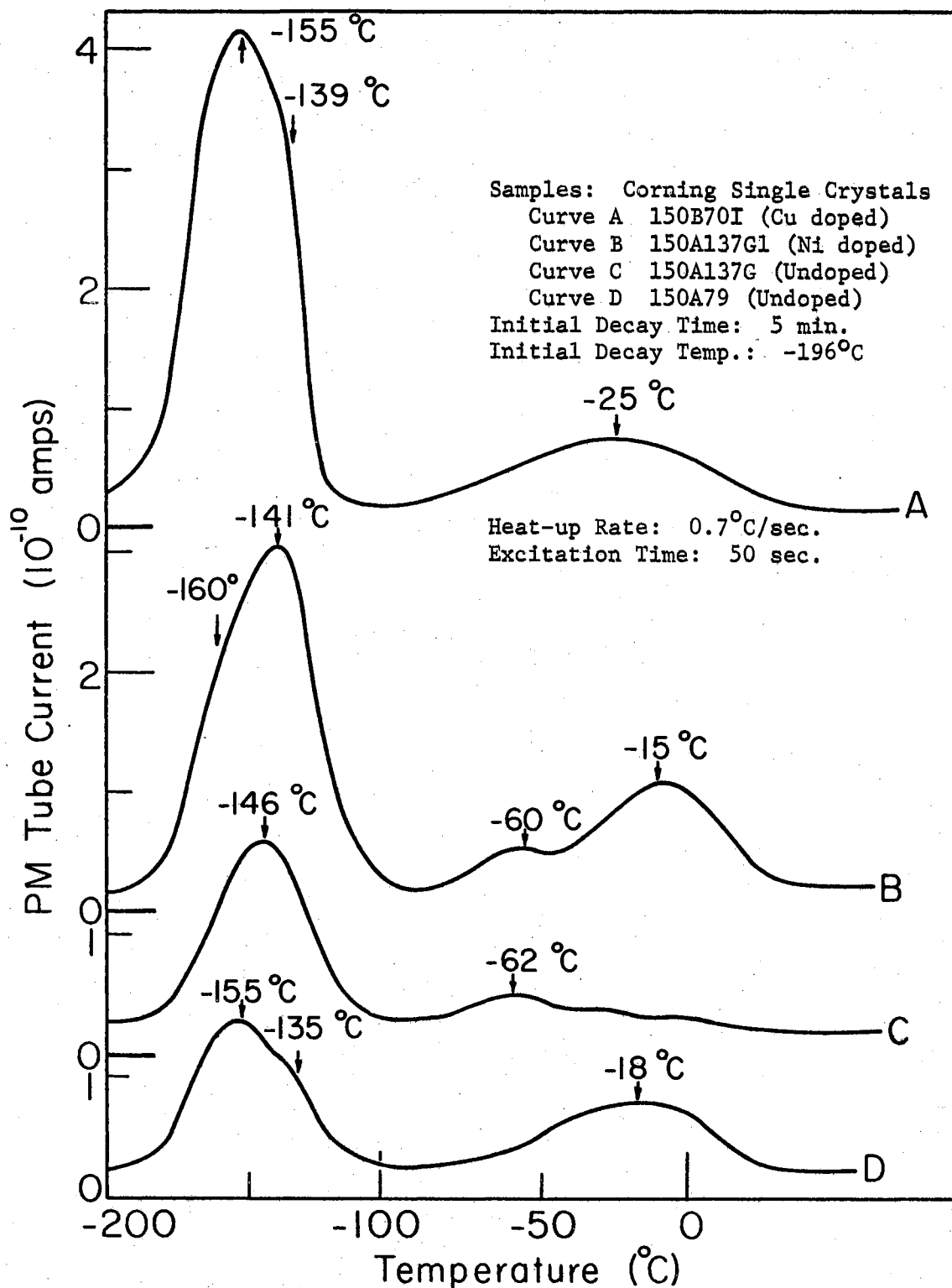


Figure 17. Representative Glow Curves of Corning Single Crystals

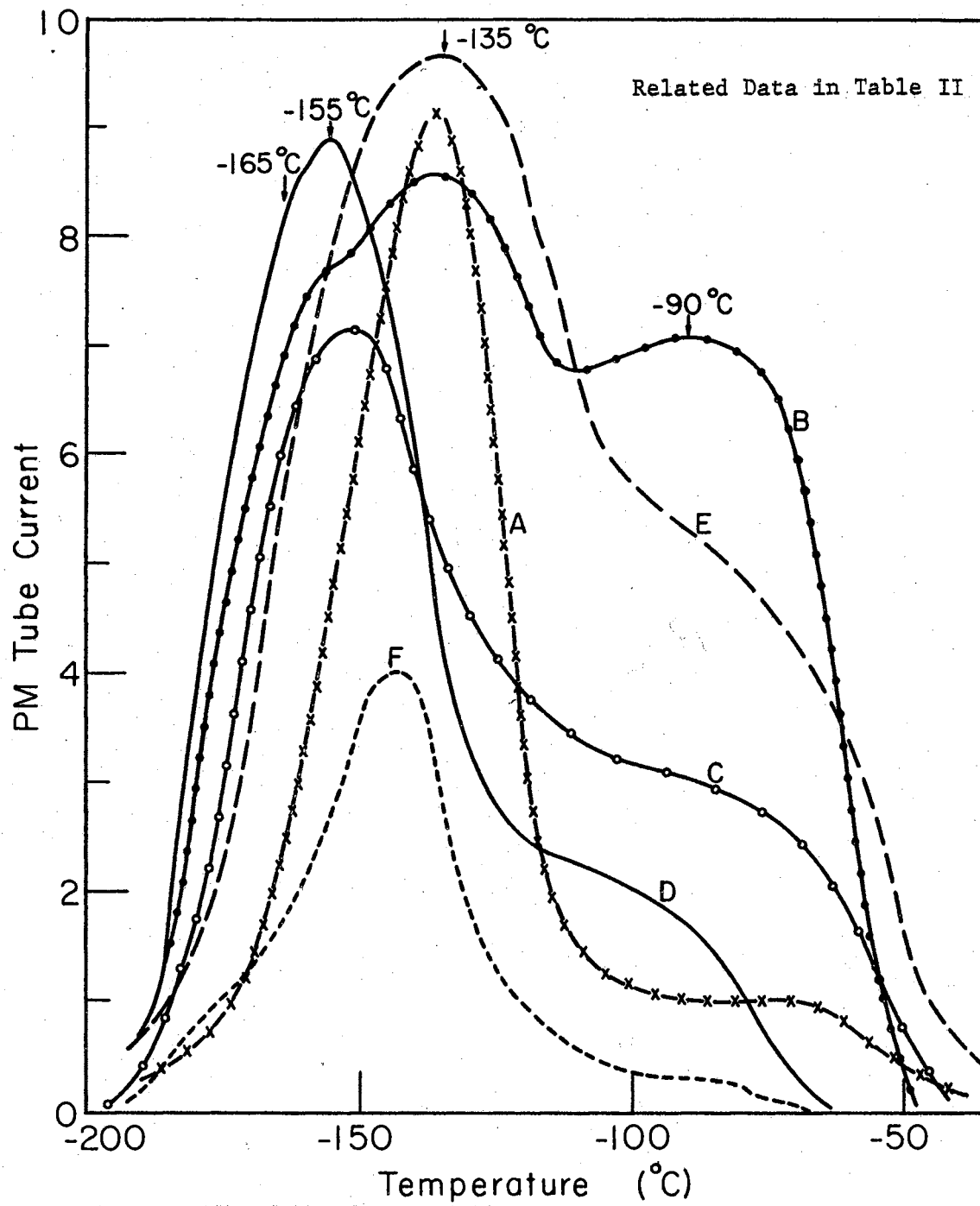


Figure 18. Representative Glow Curves of Ceramics

TABLE II

INFORMATION PERTAINING TO THE GLOW CURVES OF FIGURE 18

Curve	Sample	Initial Decay Time (min.)	Initial Decay Temp. (°C)	Heat-up Rate (°C/sec.)	Excitation Time (min.)	Peak PM Tube Current (10^{-10} amps.)
A	S-12 (0.7% Cu ₂ O)	10	-190	0.50	10	0.92
B	S-20 (0.7% ZnO)	5	-196	0.60	10	430
C	#34 (10% ZnO)	10	-196	0.55	10	720
D	#37 (Undoped)	5	-196	0.50	5	89
E	#91 (Undoped)	5	-196	0.60	5	97
F	S-8 (Undoped)	10	-196	0.12	10	40

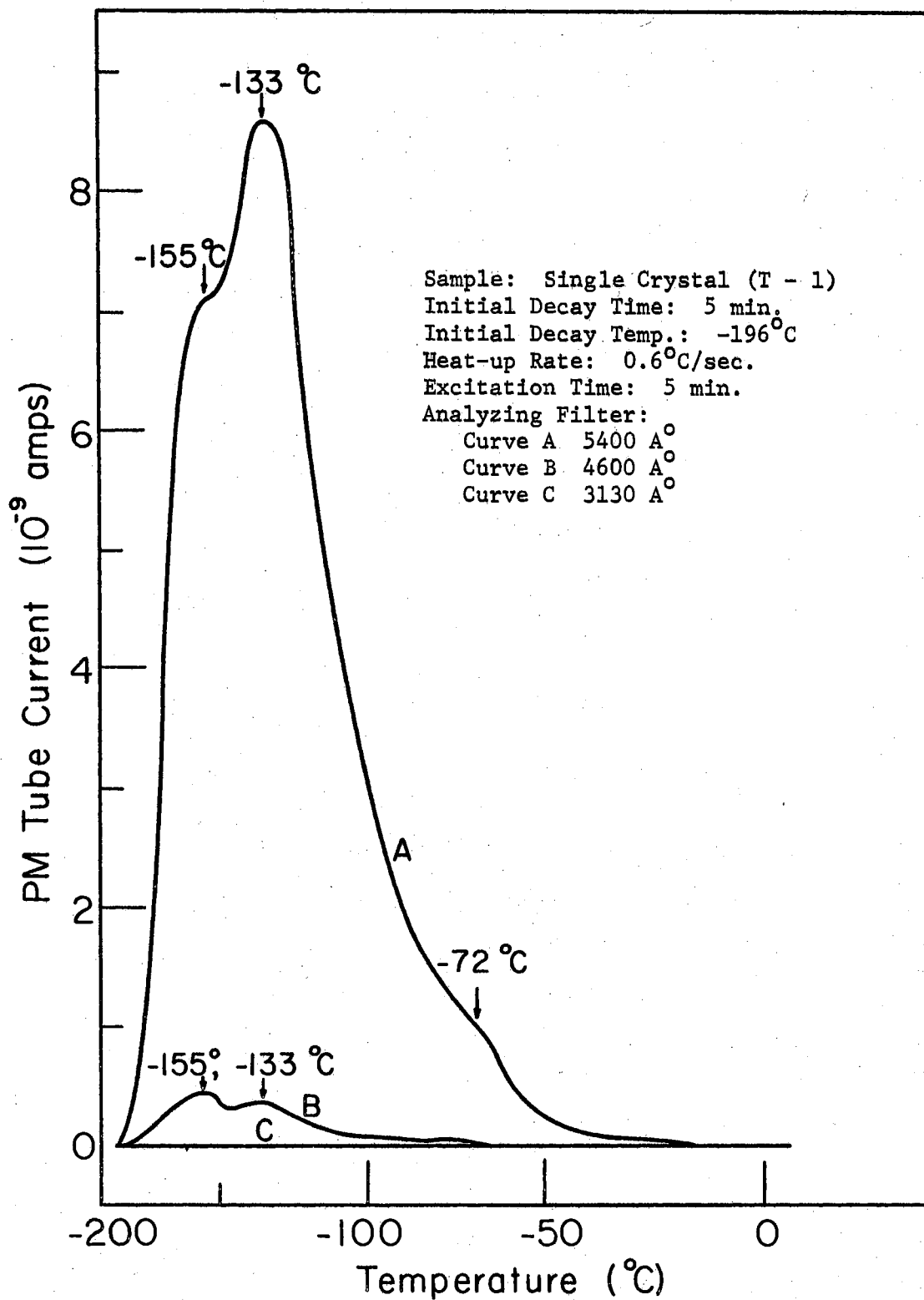


Figure 19. Spectral Distribution of Luminescence Radiation

was observed when the plane of polarization of the Glan-Thompson prism (used as an analyzer) was either perpendicular or parallel to the single crystals c-axis. These observations were made on both locally-grown and Corning single crystals. The results indicate that the luminescence is preferentially polarized perpendicular to the c-axis. Table III gives the peak heights for the two directions of polarized luminescence. So that there may be no uncertainty as to the effect being observed, luminescence from a ceramic sample was also analyzed with the polarizer. There was no change in peak luminescence intensity observed. An additional check was made by rotating the crystal through 90° with respect to the photomultiplier tube axis and analyzing the luminescence once more. Again the results were the same.

Excitation Radiation

By using the same set of filters that were used to analyze the T.S.L. radiation, it was possible to excite the samples with various energy ranges of incident light. Figure 20 depicts the effects of exciting a single crystal using three different filters. When less-than-bandgap radiation is used, no glow peaks below -60°C are apparent.

Heat Treatment Studies

Table IV compares major glow peak intensities observed following heat treatment in air and heat treatment in vacuum for three different types of ceramic specimens. In general it was found that heat treatment in air for ceramic samples would decrease the light sum (area under the glow curve) for all peaks. However, there appears to be a slight tendency for the higher temperature peaks to decrease more than those at

TABLE III
 INTENSITY OF LUMINESCENCE WITH E VECTOR POLARIZED PARALLEL
 AND PERPENDICULAR TO C-AXIS OF SINGLE CRYSTAL

Sample	Heat-up Rate °C/sec	$L_{\text{max.}}$ (10^{-10} amps.)	Polarization of E Vector Relative to C-Axis
Corning	0.75	1 and 0.5	⊥
Single	0.73	0.9 and 0.4	⊥
Crystal (150A79)	0.68	0.25 and 0.1	
	0.70	0.2 and 0.05	
	0.68	0.8 and 0.4	⊥
	0.70	0.8 and 0.4	⊥
Undoped			
Ceramic (#37)	0.73	110	Relative to PM Tube Axis
	0.73	110	
Locally -	0.70	1.5	⊥
Grown	0.61	1.0	⊥
Single	0.79	0.7	
Crystal (T-1)	0.75	0.8	
	0.79	1.4	⊥
	0.75	0.6	
Locally -	0.75	7.3	
Grown	0.66	6.3	
Crystal (G-27)	0.75	14	⊥
	0.75	14	⊥

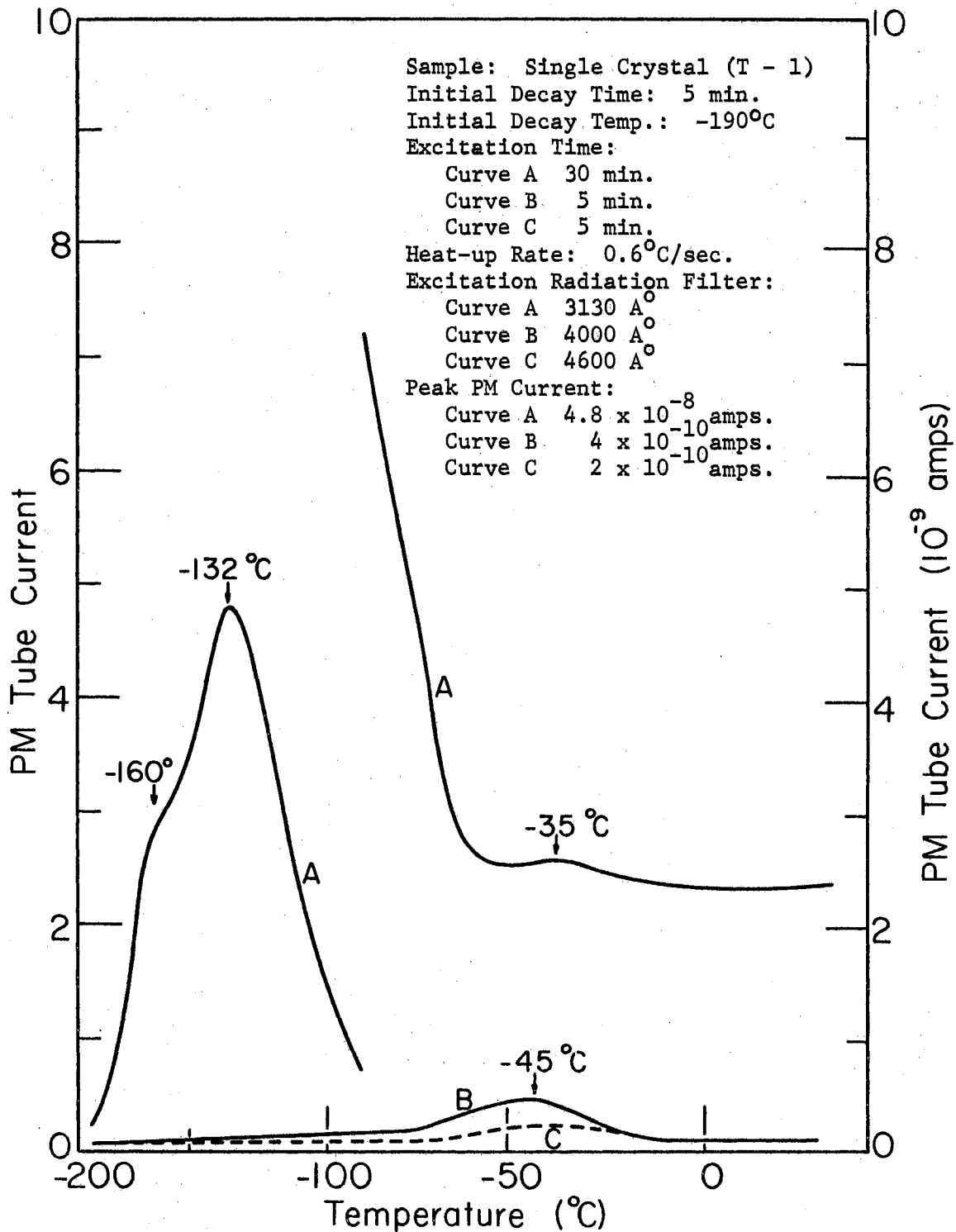


Figure 20. Glow Curves for Single Crystal Excited with Different Spectral Ranges of Radiation

TABLE IV

EFFECT OF HEAT TREATMENT ON THE MAXIMUM LUMINESCENCE INTENSITY OF CERAMICS

Sample	Heat Treated in						Heat-up Rate °C/sec.	T.S.L. Run #	
	Air			Vacuum					
	L _{max} (10 ⁻¹⁰ amps.)			L _{max} (10 ⁻¹⁰ amps.)					
	-140°C	-88°C	Ratio	-140°C	-88°C	Ratio			
Undoped (S-8)				37	5	7.4	0.10	168	
				37	5	7.4	0.10	169	
		22	2.3	9.6			0.10	170	
		12	1.2	10			0.11	171	
					26	3.2	8.1	0.11	172
		120	43	2.8			0.70	211	
0.7% ZnO (S-20)				180	74	2.4	0.68	213	
		420	350	1.2			0.65	222	
				450	420	1.0	0.62	224	
		92	70	1.3			0.13	223	
	(S-18)			100	80	1.2	0.12	225	
	(S-18)	45			66		0.12	162	
0.7% Cu ₂ O (S-13)							0.13	163	
				1.3			0.50	182	
		0.5					0.50	183	
	0.28					0.50	184		

lower temperature as is indicated by the ratios in Table IV. Zinc doping increased luminescence while copper doping significantly decreased it. On the other hand, it was found for single crystal samples that no appreciable change occurred in the light sums between the heat treatments. This is interpreted in terms of the smaller surface area of single crystals as compared to ceramic specimens.

CHAPTER V

DISCUSSION AND CONCLUSIONS

Introduction

It will be seen in the following discussion that distinct parallels can be drawn between T.S.L. and T.S.C. observations. This leads to the proposal of a relatively simple model for T.S.L. in stannic oxide which is consistent with the models proposed by others^{9,18} based on T.S.C. measurements alone.

After use of a band model has been justified, evidence for the properties and locations of electron trapping and recombination levels is discussed. Activation energies are calculated for these centers and heat treatment effects are explained in terms of the presence of chemisorbed oxygen.

Justification of Band Model

In order to invoke the band model it is necessary that there be free carriers associated with that part of the luminescence cycle wherein electrons or holes are thermally excited from trapping centers. The most direct evidence of the presence of free carriers during this part of the cycle is the comparison of T.S.L. and T.S.C. data. Houston⁹ reported T.S.C. peaks at -130°C , -80°C and -30°C for locally-grown single crystals. Matthews¹⁸ found T.S.C. peaks at -80°C and near 0°C for zinc-doped ceramic samples. Lower temperature peaks were not reported in

either of these cases, probably due to the inability to obtain sufficiently low sample temperatures. Recently Freeman⁹⁶ has been able to extend Matthews' T.S.C. measurements to lower temperatures and has revealed that lower temperature peaks do exist. Figure 21 gives a T.S.C. graph representative of his measurements on a zinc-doped ceramic sample. It will be noticed that not only are the peak temperatures very nearly the same but the relative peak heights are comparable to those of the T.S.L. glow curves. The only significant difference is the presence of a T.S.C. peak at $+57^{\circ}\text{C}$. This peak is difficult to resolve experimentally at this time because of the high level of dark current present at the higher temperatures. On the basis of these facts it is clearly appropriate to analyze stannic oxide luminescence in terms of the band model.

Trapping and Recombination Centers

It has been rather well established by thermoelectric power¹⁷ and Hall effect measurements¹⁴ that stannic oxide is an n-type semiconducting material. Recognizing this fact and maintaining consistency with the models used to explain the T.S.C. data referred to in the preceding section, one is led to the conclusion that the centers being emptied during the T.S.L. process are electron traps. Consequently the T.S.L. radiation arises from electrons making transitions from the conduction band to recombination energy levels lying in the forbidden gap.

From the basic T.S.L. measurements there appear to be at least five different electron trapping levels. It was possible to calculate activation energies from only the four lowest temperature peaks. The -15°C peak was too small to permit any calculations. Indications are that these trapping centers do not have discrete energy states but are

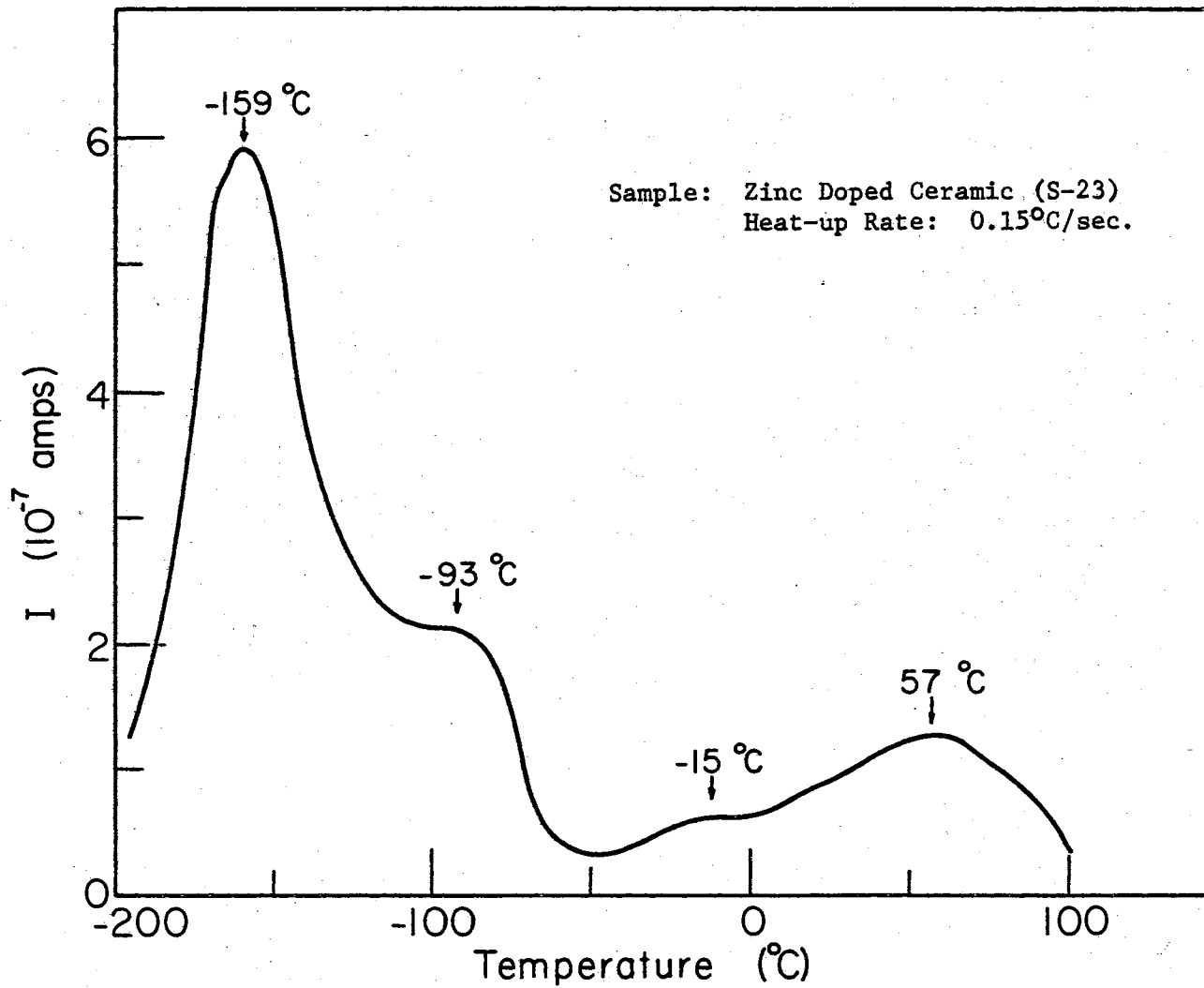


Figure 21. Thermally Stimulated Current of Ceramic Sample

spread over narrow energy bands. The principal facts which suggest this are the following: 1) There are no breaks in the slope of the initial rise curves for these peaks but instead a steady change in initial slope as the partial thermal decay is carried to higher temperatures. 2) The glow peaks shift to higher temperatures as the samples undergo increasingly higher thermal decays. That this indicates nondiscrete energy states was first suggested by Randall and Wilkins³¹. 3) The studies made by Marley and Dockerty⁹⁷ on Corning single crystals give evidence of impurity-level transport that increases as the number of oxygen vacancies is increased. This is a strong indication that the interaction between imperfection energy states can be sufficiently large to permit individual energy states to become broadened into narrow bands. It should be emphasized that all activation energies reported here were obtained using the initial rise method.

Although the presence of four low temperature glow peaks appears to imply four discrete or narrow-banded trapping levels, it was found impossible in the present work to resolve them distinctly. In practice, one energy range could be found for activation energies associated with the -160° and -135°C glow peaks and another for those associated with the -90° and -60°C peaks. The broadest spread was found for zinc-doped specimens.

Table V gives the results for several representative samples. It details the experimental range of maximum thermal decay temperatures used, the range of corresponding glow peak temperatures observed for the paired overlapping peak ranges above, and the calculated activation energy value ranges obtained by applying the initial rise method to successively decayed peaks.

TABLE V

ACTIVATION ENERGIES OF ELECTRON TRAPS
CALCULATED FROM T.S.L. MEASUREMENTS

Sample	Range of Max. Partial Decay Temperatures (°C)	Range of Decayed Peak Temperatures (°C)	Range of Calculated T.S.L. Activation Energies (eV.)
Undoped Ceramic (S-9)	-196 to -157 -116 to -106	-140 to -133 -88	0.10 to 0.16 0.19 to 0.20
Undoped Ceramic (S-8)	-190 to -168 -114 to -105	-146 to -133 -83	0.10 to 0.16 0.27
Undoped Ceramic (#37)	-184 to -143 -117 to -98	-165 to -137 -102 to -93	0.11 to 0.16 0.18 to 0.24
0.7% ZnO (#91)	-196 -114 to -53	-151 to -122 -77 to -49	0.08 to 0.10 0.18 to 0.30
Single Crystal (T - 1)	-196 to -147 -145 to -83	-165 to -118 -119 to -42	0.11 to 0.17 0.18 to 0.25

For the sake of comparison, trapping level activation energies calculated from T.S.C. data by other experimenters are given in Table VI. Values for the low temperature peaks correlate favorably with those in Table V. It must be recognized that T.S.C. peaks suffer from a lack of resolution similar to that found for T.S.L. peaks. No T.S.L. glow peaks which might correspond to the T.S.C. peaks above -15°C have yet been observed.

The location within the energy gap of the imperfection energy states associated with the recombination centers is calculated from the wavelength of the luminescence radiation. Visually matching its yellowish color with a known spectral source and observing the fact that most of it passed through a 5400 \AA filter as described in Chapter III, the energy of the recombination radiation is judged to be about 2.2 eV. Jeges¹⁶ also reports a yellowish recombination radiation observed in the electroluminescence of stannic oxide single crystals. It was found to be affected to only a small degree by the various dopants such as copper, silicon, lead, cobalt and manganese.

Since the recombination radiation energy and the structure (although not the intensity) of the low temperature glow peaks are apparently little affected by the dopant, it would seem that the centers responsible for these effects arise from intrinsic defects or other impurities than those intentionally added. Such imperfections would normally be expected to be widely dispersed through the bulk of the crystals. For the recombination centers in particular, it should be noted that the output radiation is in the wavelength range for high optical transmission and that its polarization direction corresponds to a crystal symmetry axis. These facts are consistent with bulk locations for the imper-

TABLE VI

ACTIVATION ENERGIES OF ELECTRON TRAPS
CALCULATED FROM T.S.C. MEASUREMENTS

Sample	Peak Temperatures (°C)	Activation Energy (eV)	Reference
Single Crystals (Locally-Grown)	-120	0.21	Houston ⁹⁷ (p. 119)
	-15	0.5	
	+60	0.6	
Ceramics (0.7% ZnO)	-140	0.09 to 0.12	Freeman ⁹⁶
	-80	0.12 to 0.20	
	0	0.54	Matthews ¹⁸ (p. 69)
+60	0.64		

fections involved.

An interesting correlation between the T.S.L. data and optical quenching measurements lends additional support to the placement of a recombination center roughly midway in the optical band gap. Houston and Kohnke's optical quenching data indicate a break from a steady rise in percent optical quenching starting at 6500 \AA° (1.9 eV) and a leveling off at 5500 \AA° (2.25 eV).⁹⁸ For wavelengths below 5500 \AA° the percent optical quenching continues to decrease. In the basic optical quenching process⁹⁹, holes are effectively transferred from sensitizing centers (1.3 eV above the valence band in work reported in reference⁹⁸) to the recombination centers reducing carrier lifetime and quenching the photoconductivity. However, if the excitation energy of the extrinsic source is increased until it is possible to excite electrons directly into the recombination centers from the valence band, the carrier lifetime will once again increase and percent optical quenching start to decrease. The break in the curve described above is now tentatively assigned to the onset of the second process. Adding this 1.9 eV as the energy of the recombination centers above the valence band and 2.2 eV from the preceding paragraphs as the energy of recombination centers below the conduction band gives 4.1 eV as the optical bandgap, in excellent agreement with other determinations⁷.

Heat Treatment Effects

From the heat treatment experiments it appears that chemisorption of gases on the samples decreases the output light sum. If the trapping and radiative recombination centers are located in the bulk of the specimen, then the number of these centers should not be affected by the

relatively low temperature of the heat treatments used in this study. However, the number of surface centers could be greatly changed. Consequently, indications are that upon heat treating in air the presence of chemisorbed gases provides nonradiative centers or centers that radiate outside the visible range. Nyberg and Colbow¹⁰⁰ have demonstrated that chemisorbed oxygen decreases the photoluminescence efficiency in cadmium sulfide. They explain this effect by considering chemisorbed oxygen as given rise to nonradiative recombination centers. Matthews¹⁸ has shown that oxygen is one of the active species in chemisorption on stannic oxide and that nitrogen produces no apparent effect. Houston⁹⁷ gives evidence that water vapor also has a quenching effect on the photoresponse of single crystals. Ceramic samples were the only ones to show any consistent behavior of luminescence change with heat treatment. The single crystals apparently did not have sufficiently large surface-to-volume ratios to provide for significant changes upon gas adsorption.

As an alternative experiment suitable for single crystals, the maximum luminescence intensity was observed for air heat-treated samples exposed to the incident radiation for equal periods of time, as a function of integrated total exposure time. A steady increase of peak height was noted with increased total exposure time. This effect is interpreted again as being caused by reduction in the number of non-radiative surface recombination centers. Here, however, the removal of adsorbed gas was accomplished by a photodesorption process rather than by thermal desorption.

In Table IV it was noted that the ceramic specimen higher temperature peaks were affected to a greater degree by heat treatment than were

the lower temperature peaks. This is believed to be due to the fact that the higher temperature peaks are associated with trapping centers that lie physically closer to the surface than those associated with the lower temperature peaks. Similar considerations based on changes in T.S.C. peaks and continuous thermal quenching magnitudes, led Houston⁹⁷ to argue that the lower temperature peaks observed in single crystals were also associated with centers lying with the bulk.

Summary of Model

Various points of the model proposed to explain T.S.L. results in stannic oxide will now be summarized. The experimental evidence to support each point of the model is briefly identified. A pictorial representation of this model is given in Figure 22.

- 1) The luminescence arises from electronic transitions between conduction band energy states and a recombination level in the forbidden gap. (Similarity of T.S.C. and T.S.L. data. Observation of n-type conductivity.)
- 2) There are at least 5 different electron trapping levels. The -160°C and -135°C peaks are associated with neighboring levels that appear to be narrow overlapping bands lying between 0.08 eV and 0.17 eV below the conduction band. Likewise the -90°C and -60°C peaks are associated with overlapping levels that lie between 0.18 eV and 0.30 eV below the conduction band. (Initial rise calculations for partially thermally decayed T.S.L. measurements)
- 3) There is an electron trapping level lying about 0.50 eV below the conduction band. This is associated with the -15°C glow

peak. (T.S.L. and T.S.C.)

- 4) The radiative recombination centers lie about 2.2 eV below the conduction band. (Spectral analysis of T.S.L. radiation) and about 1.9 eV above the valence band. (Optical quenching)
- 5) There exist nonradiative surface recombination states which are due to the presence of chemisorbed oxygen or water vapor. (T.S.L. Heat treatment studies)
- 6) The intrinsic optical bandgap is about 4.0 eV. (Photoconductivity)

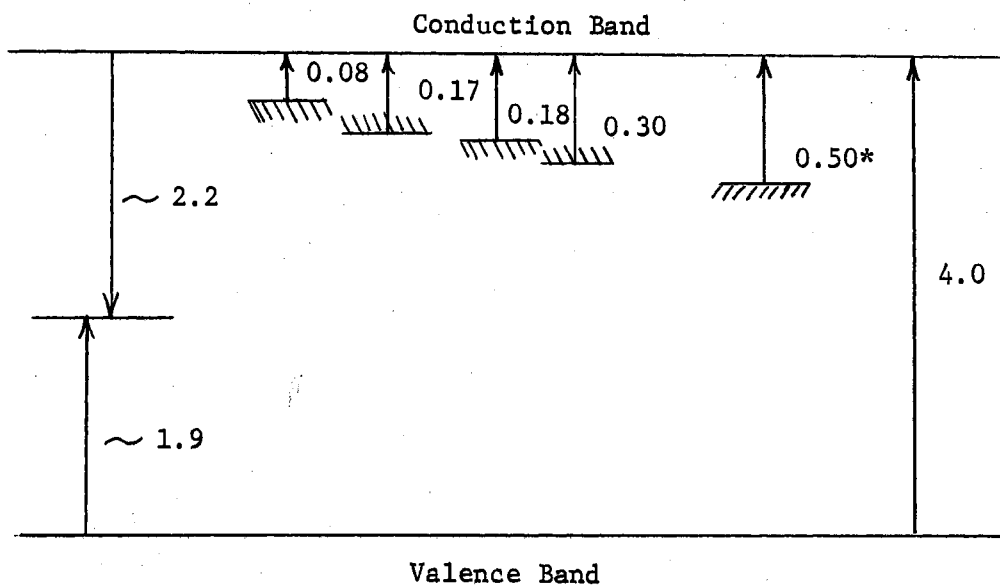


Figure 22. Energy Level Diagram of Model Proposed for Stannic Oxide (*From T.S.C. Measurements⁹⁷)

Suggestions for Further Study

The most obvious area for further work involves finding a means of controlling the experimental technique to obtain better resolution of the glow peaks. First attempts would increase specimen size, reduce excitation time, and retain low heat-up rates. Calculation methods

other than the initial rise method should be tested. Additional T.S.C. data should be obtained to allow more complete correlation of information obtained from the two types of experiments.

There are several other specific areas that deserve further investigation. One is a determination of the identity of the various centers. Also, more conclusive information is needed about the physical location of these centers. A more refined spectral analysis of the luminescence radiation is in order and additional heat treatment studies should be made. The following suggestions are offered as possible ways of making these investigations.

Information concerning both the location and nature of the trapping levels in magnesium oxide has been found by comparing electron spin resonance and T.S.L. data. Hansler and Segelken have described experimental techniques that should also be applicable to stannic oxide when the centers are due to foreign ions¹⁰¹.

Some of the centers may be due to intrinsic defects. This possibility could be checked out by heat-treating samples at temperatures above 1000°C. In this manner the density of oxygen vacancies could be varied and the T.S.L. studied as a function of oxygen vacancy density.

In the work reported here only a rough spectral analysis was made of the T.S.L. radiation. It was not sensitive enough to detect any small changes that might be induced by the presence of various impurities. It would be of value to make more refined analysis of this radiation, not only to observe the effect of impurities, but also to obtain a more accurate determination of the energy level location of the recombination centers with respect to the conduction band. An experimental arrangement similar to that used by Halperin and

Kristianpoller would be of value here.⁹⁵

The effects of the presence of chemisorbed gases could be investigated by several methods. The kinetics of phosphorescence decay following a rapid increase of ambient gas pressure at liquid nitrogen temperature should give insight into the mechanism of nonradiative surface recombination. Heat treatments should be carried out in both donor and acceptor-type gases to determine the resultant effect on the nature of the glow curves. The T.S.L. experiment itself could be done with the sample in an atmosphere of dry gas rather than in a vacuum.

A final suggestion for an experiment that would be of use in determining how traps may be filled is to study the T.S.L. as a function of the wavelength of the excitation radiation. Preliminary measurements indicate that it is possible by using extrinsic radiation to fill the 0.5 eV traps without filling shallower traps. If this is correct, it implies that it is possible to excite electrons into these traps without their passing through the conduction band. However, an experiment using more nearly monochromatic radiation is necessary in order to establish this fact.

BIBLIOGRAPHY

BIBLIOGRAPHY (Continued)

(1967).

19. Miloslavskii, V. K., S. P., *Optics and Spectroscopy*, 7, 154 (1959).
20. Bauer, G., *Ann. Physik*, 30, 433 (1937).
21. Fisher, A., *Z. Naturforsch*, 9a, 508 (1954).
22. Arai, T., *J. Phys. Soc. Japan*, 15, 916 (1960).
23. Miloslavskii, V. K. and Tyashenko, S. P., *Optics and Spectroscopy*, 8, 455 (1960).
24. Kuznetsov, A. Ya., *Soviet Phys. Solid State*, 2, 35 (1960).
25. Aitchison, R. E., *Aust. J. Appl. Sci.*, 5, 10 (1954).
26. Foex, M., *Bull. Soc. Chim. France*, 11, 6 (1944).
27. Marley, J. A. and MacAvoy, T. C., Investigation of the Mechanism of Single Crystal Growth in High Temperature System. Final Report, June 1961 - June 1962, Contract No. AF 19(604)-8447.
28. Kroeger, F. A., *Physica*, 14, 425 (1948).
29. Pringsheim, P., Fluorescence and Phosphorescence, Interscience Publishers, New York (1949).
30. Curie, D., Luminescence in Crystals, John Wiley and Sons, New York (1963).
31. Randall, J. T. and Wilkins, M. H. F., *Proc. Roy. Soc. (London)*, A184, 366 (1945).
32. Garlick, G. F. J., "Luminescence", Handbuch der Physik, 26, 2 Springer, Berlin (1958).
33. Stokes, G. Q., *Phil. Trans. Roy. Soc. (London)*, A142, II, 463 (1852).
34. Becquerel, E., La Lumiere, ses Causes et ses Effets, Gauthier-Villars, Paris (1867).
35. Jablonski, A., *Nature*, 131, 839 (1933).
36. Seitz, F., *J. Chem. Phys.*, 6, 150 (1938).
37. Mott, N. F., *Proc. Roy. Soc. (London)*, A171, 27 (1939).
38. Riehl, N. and Schon, M., *Z. Physik*, 114, 682 (1939).

BIBLIOGRAPHY (Continued)

39. Johnson, R. P., J. Opt. Soc. Am., 29, 387 (1939).
40. Urbach, F., Wien. Ber. IIa, 139, 473 (1926).
41. Garlick, G. F. J. and Gibson, A. F., Proc. Roy. Soc. (London), A60, 574 (1948).
42. Booth, A. H., Canad. J. Chem., 32, 214 (1954).
43. Halperin, A. and Braner, A. A., Phys. Rev., 117, 408 (1960).
44. Hill, J. J. and Schwed, P. M. J. Chem. Phys., 23, 652 (1955).
45. Gobrecht, H. and Hofmann, D., J. Phys. Chem. Solids, 27, 509 (1966).
46. Broser, I. and Broser-Warminsky, R., Brit. J. Appl. Phys., 6, Suppl. 4, S90 (1955).
47. Halperin, A. and Chen, R., Phys. Rev., 148, 839 (1966).
48. Schon, M., Techn. Wiss. Abh. Osram Ges., 7, 175 (1958).
49. Braunlich, P., Paper in Proceedings of the Conference on the Applications of Thermoluminescence to Geological Problems, Spoleto, Italy (1966).
50. Arbell, H. and Halperin, A., Phys. Rev., 117, 45 (1960).
51. Merz, J. L. and Pershan, P. S., Charge Conversion of Irradiated Rare-Earth Ions in Calcium Fluoride, (1966), Contract No. Nor 1866 (16).
52. Wertz, J. E. and Coffman, R. E., J. Appl. Phys., 36, 2959 (1965).
53. Halperin, A., and Nahum, J., J. Phys. Chem. Solids, 18, 297 (1961).
54. Oster, G. and Yamamoto, M., J. Appl. Phys., 37, 823 (1966).
55. Kroeger, F. A. and Dikhoff, J. A. M., J. Electrochem. Soc., 99, 144 (1952).
56. Williams, F. E. and Eyring, H., J. Chem. Phys., 15, 289 (1947).
57. Gurney, R. W. and Mott, N. F., Trans. Faraday Soc., 35, 69 (1937).
58. Williams, F. E., J. Opt. Soc. Am., 39, 648 (1949).
59. Kroger, F. A., Hoogenstaaten, W., Bottema, M. and Botden, P. J., Physica, 14, 81 (1948).
60. Kroeger, F. A. and Dikhoff, J. A. M., Physica, 16, 297 (1950).

BIBLIOGRAPHY (Continued)

61. Prener, J. S. and Williams, F. E., *J. Electrochem. Soc.*, 103, 342 (1956).
62. Leverenz, H. W., *Luminescence of Solids*, John Wiley and Sons, New York (1950).
63. Shannon, R. D., *J. Appl. Phys.*, 35, 3414 (1964).
64. Hurlen, T., *Acta Chem. Scand.*, 13, 365 (1959).
65. Kingery, W. D., *Introduction to Ceramics*, John Wiley and Sons, New York (1960).
66. Markham, J. J. and Seitz, N. F., *Phys. Rev.*, 74, 1014 (1948).
67. Ghormley, J. A. and Levy, H. A., *J. Phys. Chem.*, 56, 548 (1952).
68. Pauling, L., *The Nature of the Chemical Bond*, Cornell University Press, New York (1960).
69. Grant, F. A., *Rev. Mod. Phys.*, 31, 646 (1959).
70. Frederikse, H. P. R., *et. al.*, Paper in *Semiconductor Materials*, Soviet Conference on Problems of Metallurgy and Physics of Semiconductors, 4th Edition, ed. N. Kh. Abrikosov.
71. Doerffler, W. and Hauffe, K., *J. of Catalysis*, 3, 156 (1964).
72. Mark, P., *J. Phys. Chem. Solids*, 26, 959 (1965).
73. Moore, G. E. and Unterwald, F. C., *J. Chem. Phys.*, 40, 2626 (1964).
74. Stone, F. S., *Advances in Catalysis*, 13, 1 (1962).
75. Melnick, D. A., *J. Chem. Phys.*, 26, 1136 (1957).
76. Moglich, F. and Rompe, R. W., *Z Physik*, 115, 707 (1940).
77. Goodman, B., Lawson, A. W. and Schiff, L. I., *Phys. Rev.*, 71, 191 (1947).
78. Curie, D., *J. Phys. et Radium*, 12, 920 (1951).
79. Kubo, R., *Phys. Rev.*, 86, 929, (1952).
80. Haung, K. and Rhys, A., *Proc. Roy. Soc. (London)*, A204, 406 (1950).
81. Vasileff, H. D., *Phys. Rev.*, 96, 603, (1954).
82. Curie, M. and Curie, D., *Cahier de Physique*, 57, 52 (1955).

BIBLIOGRAPHY (Continued)

83. Braunlich, P., J. Appl. Phys., 38, 2516 (1967).
84. Keating, P. N., Proc. Phys. Soc. (London), 78, 1408 (1961).
85. Lushik, Ch. B., Dok. Akad. Nauk. SSR, 101, 641 (1955).
86. Unger, K., Abh. Deutsch. Akad. Wiss., 7, 170 (1960).
87. Grossweiner, L. J., J. Appl. Phys., 24, 1306 (1953).
88. Kelly, P. J. and Laubitz, M. J., Can. J. Phys., 45, 311 (1967).
89. Hoogenstaaten, W., Phil. Res. Rept., 13, 515 (1958).
90. Urbach, F., Mat. Natur., 139, 353 (1930).
91. Nicholas, K. H. and Woods, J., Brit. J. Appl. Phys., 15, 783 (1964).
92. Kunkle, H. F., Ph.D. dissertation, Oklahoma State University (1966).
93. Marley, J. A. and MacAvoy, T. C., J. Appl. Phys., 32, 2504 (1961).
94. Matthews, H. E., Master's Thesis, Oklahoma State University (1965).
95. Halperin, A., and Kristianpoller, N., J. Opt. Soc. Am., 48, 996 (1958).
96. Freeman, J. A., Private Communication (1968).
97. Houston, J. E., Photoelectronic Analysis of Imperfections in Grown Stannic Oxide Crystals, Tech. Rept. #4, Feb. 1965, Contract #Nor-2595(01).
98. Houston, J. E. and Kohnke, E. E., J. Appl. Phys., 37, 3083 (1966).
99. Bube, R. H., Photoconductivity of Solids, John Wiley and Sons, New York (1960).
100. Nyber, W. D. and Colbow, K., Can. J. Phys., 45, 2833 (1967).
101. Hansler, R. L. and Segelken, W. G., J. Phys. Chem. Solids, 13, 124 (1960).

VITA

3

Robert Don Eagleton

Candidate for the Degree of
Doctor of Philosophy

Thesis: A STUDY OF THERMALLY STIMULATED LUMINESCENCE IN STANNIC OXIDE

Major Field: Physics

Biographical:

Personal Data: Born in Ladonia, Texas, August 19, 1937, the son of Mr. and Mrs. Winslow F. Eagleton.

Education: Graduated from Bonham High School, Bonham, Texas, May, 1955; attended Abilene Christian College, Abilene, Texas, from 1955 to 1959, received the Bachelor of Science degree with a major in Physics; received the Master of Science degree from Oklahoma State University in 1962, as a National Defense Education Act Fellow, with a major in Physics; completed the requirements for Doctor of Philosophy degree at Oklahoma State University in May, 1969.

Professional Experience: Instructor, U.S. Naval Nuclear Power School, 1961 - 65; graduate teaching assistant, Physics Department, Oklahoma State University, 1966 - 68.